UNIVERSITA' DEGLI STUDI "G. d'Annunzio"
Chieti-Pescara

SCUOLA SUPERIORE "G. d'Annunzio"

DOTTORATO DI RICERCA IN NEUROSCIENZE E IMAGING

CICLO XXXVIII

ECOGRAFIA DINAMICA NEUROMUSCOLOSCHELETRICA

Dipartimento di Neuroscienze, Imaging e Scienze Cliniche

Settore Scientifico Disciplinare: MEDS-26/D, MEDS-22/A

Dottorando
(Dott. Giulio Cocco)

Coordinatore Prof.
(Prof. Carlo Sestieri)

Tutor
(Prof. Massimo Caulo)

Anni Accademici 2022/2025

Ecografia dinamica neuromuscoloscheletrica

Indice

Capitolo 1 – Introduzione

Nota metodologica

Capitolo 2 – Articoli prodotti

2.1 Ultrasound Imaging of the Sciatic Nerve

2.2 Dynamic Ultrasound Assessment for Insertional Achilles Tendinopathy: the CORI (Cocco-Ricci) Sign

2.3 Dynamic Ultrasound Imaging for Insertional Achilles Tendinopathy: a Retrospective Observational Study

Capitolo 3 – Lavori scientifici pubblicati

Capitolo 4 – Partecipazioni a congressi

Capitolo 5 – Premi e riconoscimenti

Capitolo 6 – Conclusioni

Ringraziamenti

1. Introduzione

L'ecografia ha assunto negli ultimi decenni un ruolo sempre più centrale nello studio dell'apparato neuromuscoloscheletrico (NMSK), imponendosi come metodica di primo livello per la valutazione di muscoli, tendini, nervi periferici e articolazioni. Le sue caratteristiche intrinseche – sicurezza, ripetibilità, basso costo, assenza di radiazioni ionizzanti e possibilità di utilizzo bedside – ne hanno favorito una diffusione capillare sia in ambito ospedaliero che ambulatoriale. A queste peculiarità si aggiunge una proprietà distintiva che la rende unica rispetto ad altre tecniche di imaging: la dinamicità.

L’ecografia è infatti l’unica metodica che consente di osservare le strutture anatomiche in movimento, di valutarne lo scorrimento reciproco e di correlare le immagini con manovre funzionali o con la riproduzione dei sintomi del paziente. Questa capacità di integrare la valutazione morfologica con quella funzionale costituisce un valore aggiunto determinante nell’imaging NMSK, in quanto permette di cogliere alterazioni che rimarrebbero silenti in condizioni statiche. Nonostante ciò, nella letteratura scientifica e nella pratica clinica l’ecografia è stata storicamente utilizzata in maniera prevalentemente statica, con protocolli focalizzati sulla descrizione strutturale piuttosto che dinamica.

Negli ultimi anni si è assistito a un progressivo riconoscimento dell’importanza dell’approccio ecografico dinamico. Diversi studi hanno evidenziato come le manovre dinamiche ecoguidate possano migliorare l’accuratezza diagnostica in numerose condizioni cliniche: dalle sindromi da intrappolamento nervoso, alle tendinopatie, fino agli impingement articolari e muscolari. Tuttavia, l’applicazione della dinamicità ecografica rimane ancora frammentaria, spesso affidata all’esperienza del singolo operatore e priva di protocolli sistematici e standardizzati. Tale carenza rappresenta un gap rilevante, poiché limita la riproducibilità degli esami e ne riduce l’impatto clinico e scientifico.

In questo scenario si colloca il percorso di ricerca sviluppato nel presente dottorato, dedicato alla valorizzazione dell’ecografia dinamica neuromuscoloscheletrica. L’obiettivo è stato duplice: da un lato, definire protocolli di esplorazione standardizzati che integrassero in modo strutturato l’impiego di manovre dinamiche; dall’altro, proporre e validare nuovi segni ecografici dinamici in grado di migliorare la diagnosi di patologie complesse.

Il primo contributo ha riguardato il Nervo Sciatico, il più grande nervo periferico dell’organismo, potenzialmente coinvolto in sindromi da intrappolamento extravertebrali. La letteratura disponibile descriveva in maniera incompleta la sua valutazione ecografica, in particolare per quanto riguarda

l’analisi dinamica lungo il decorso gluteo e prossimale della coscia. Il lavoro di ricerca ha permesso di proporre un protocollo ecografico standardizzato, identificando quattro finestre anatomiche di riferimento e integrando manovre dinamiche mirate a distinguere reperti fisiologici da alterazioni patologiche. Tale approccio ha dimostrato di aumentare la sicurezza diagnostica e di fornire strumenti utili nella gestione delle neuropatie non discogeniche.

Il secondo contributo ha introdotto un nuovo segno ecografico dinamico per la valutazione della tendinopatia inserzionale del tendine d’Achille (IAT): il segno CORI (Cocco-Ricci). Questo segno sfrutta il versamento della borsa retrocalcaneare profonda come “mezzo di contrasto naturale” per evidenziare, attraverso una manovra di compressione manuale, eventuali lesioni delle fibre profonde del tendine. La descrizione del segno CORI ha evidenziato come l’ecografia dinamica, opportunamente applicata, possa superare i limiti della valutazione statica in un distretto anatomico particolarmente complesso e soggetto a falsi negativi.

Il terzo studio ha avuto come obiettivo la validazione clinica del segno CORI attraverso un’analisi osservazionale retrospettiva condotta su una coorte di pazienti con diagnosi clinica di IAT. I risultati hanno confermato la rilevanza del segno, evidenziando una sua associazione con specifici pattern statici (tendinosi inserzionale, iperemia intratendinea, borsite retrocalcaneare iperemica) e dimostrando come la componente dinamica migliori la capacità diagnostica globale dell’esame ecografico.

L’insieme di questi studi ha contribuito a consolidare il valore della dinamicità ecografica nell’imaging NMSK, sottolineando come l’integrazione tra statico e dinamico consenta non solo di aumentare la sensibilità e la specificità diagnostica, ma anche di fornire indicazioni più precise per il trattamento e la riabilitazione.

Il presente dottorato si propone di dimostrare che l'ecografia dinamica NMSK non rappresenta un semplice perfezionamento tecnico, ma un vero e proprio cambio di paradigma. L'attenzione si sposta dalla mera analisi della struttura all'osservazione della funzione, dal fermo immagine al movimento, aprendo nuove prospettive non solo per la diagnostica ma anche per l'intervento terapeutico personalizzato.

Nota metodologica

La presente tesi di dottorato raccoglie i 3 principali lavori scientifici realizzati durante il triennio di ricerca, pubblicati o sottomessi alle riviste scientifiche impattate ed indicizzate sui principali database internazionali (Scopus/ Web of Science). Per garantire la fedeltà al contenuto e alla forma originaria, i capitoli che riprendono articoli già pubblicati vengono riportati in lingua inglese, così come apparsi sulle riviste di riferimento. Le sezioni introduttive, di discussione generale e di conclusione sono invece redatte in lingua italiana, al fine di offrire una cornice complessiva e unitaria al lavoro svolto.

2.1 Ultrasound Imaging of the Sciatic Nerve

INTRODUCTION

The sciatic nerve (SN) is the largest peripheral nerve of the human body. It presents sensory nerve fibers innervating a wide skin surface of the lower limb and, motor nerve fibers innervating several muscles of the pelvis, thigh, leg, and foot. The SN originates from the ventral rami of spinal nerves L4 through S3 and contains fibers from both the posterior and anterior divisions of the lumbosacral plexus. [1] Crossed the intervertebral foramina, the nerve roots converge in a single peripheral nerve. [2]

The SN crosses the greater sciatic foramen inferiorly to the piriformis muscle **(Figure 1)** along with the pudendal nerve, inferior gluteal nerve, nerve to obturator internus muscle, nerve to quadratus femoris muscle, and the posterior femoral cutaneous nerve. [1; 2] The anatomical portion of the greater sciatic foramen inferior to the piriformis muscle is defined as infrapiriform foramen **(Figure 2)** where also the internal pudendal vessels and inferior gluteal vessels are located **(Table 1)**. Instead, the suprapiriform foramen is crossed by the superior gluteal nerve and superior gluteal vessels. Passed the infrapiriform foramen, the SN runs below the gluteus maximus muscle inside an anatomical area known as the deep gluteal space. [3] At this level, the SN is protected from the sacrum by the pyramidalis muscle, and more caudally from the ischium by the superior gemellus and inferior gemellus muscles, the obturator internus muscle, and the quadratus femoris muscle **(Figure 3)**. [4] Interestingly, superior gemellus, inferior gemellus, and obturator internus are collectively defined as the *triceps coxae*. The segment of SN located in the deep gluteal space normally shows a (gentle) curvilinear shape to wrap the muscle belly of triceps coxae after exiting from the infrapiriform foramen. [5] More caudally, the SN reaches the proximal third of the thigh running within the interfascial plane between the hamstrings muscle complex and the adductor magnus muscle **(Figure 1)**. [6] Unlike the gluteal segment, the SN shows a linear course in the proximal thigh below the long head of the biceps femoris. [5]

Lastly, before reaching the popliteal fossa, it splits into 2 main branches **(Figure 1)** i) the tibial nerve directed towards the posterior compartment of the leg and, ii) the common peroneal nerve which runs towards the anterolateral compartment of the leg. [2]

SCANNING TECHNIQUE

With the patient prone, a pillow can be positioned under the pelvic region to passively flex the hip and optimize the ultrasound assessment of the SN at the passage along the inferior gluteal fold reducing its anisotropy. Likewise, a neutral rotation of the hip is suggested to avoid an overstretch

of the nerve in the deep gluteal space and accurately assess its perfusion pattern. Usually, a linear probe with a wide range of frequency (e.g., 5-18 Mhz) can be used to evaluate the SN also in patients with a large body habitus. The hypoechoic fascicles and hyperechoic interfascicular epineurium define the typical honeycomb structure in transverse scan and fascicular pattern in longitudinal view. [7] Comparative scanning should be always performed to correctly interpret the pathological sonographic findings and the cross-sectional area of the nerve. Moreover, the authors suggest performing each and every patient the Color/Power doppler assessment to visualize both the perineural vascular structures and the perfusion pattern of the SN. [7].

In order to standardize the sonographic assessment of the SN we suggest using four main reference anatomical zones which are most commonly involved in pathological conditions – infrapiriform foramen, ischial tuberosity region, ischiofemoral space, and proximal thigh.

Infrapiriform foramen

Using a longitudinal oblique plane, the SN can be observed, in the long axis, passing under the inferior edge of the piriformis muscle and traveling over the triceps coxae **(Figures 1B & 2)**. The latter presents two hypoechoic muscle bellies - the superior and inferior gemellus - and a hyperechoic connective portion of the obturator internus tendon **(Figure 4A)**. In physiological conditions, the SN at this level presents a slightly curved course and the fascicular pattern can be clearly visualized along its entire course.

The most common pathological sonographic finding is the “dive sign” related to a mechanical entrapment of the SN in between the piriformis and the triceps coxae **(Figure 4B)**. Indeed, the spatial deformation of the infrapiriform foramen secondary to the shortening and/or thickening of the aforementioned muscles leads to an abrupt bending of the SN which appears markedly hypoechoic (due to anisotropy) losing its classical fascicular pattern. At this level, shifting the probe more

distally, a thick hyperechoic interfascial plane can be easily observed and used as an anatomical landmark to promptly differentiate the quadratus femoris muscle from the inferior gemellus muscle **(Figure 4C)**. For sure, several anatomical variations can be encountered in clinical practice with a single SN or multiple neural branches traveling within the infrapiriform foramen, suprapiriform foramen, but also inside the muscle belly of the piriformis muscle as well. [4 ; 8] Interestingly, bending of the SN in the deep gluteal space can also be related to hip internal rotation and isometric contraction of the triceps coxae, due to the presence of a connective anchorage between the nerve and the obturator internus tendon – i.e., a neural pulling mechanism. [6 ; 9] In this sense, to correctly interpret the aforementioned "dive sign", it should always be coupled with the clinical findings and evaluated in a neutral position of the hip without active contraction of the external rotator muscles.

Ischial tuberosity region

Using a transverse scan, the bony cortex of ischial tuberosity can be easily identified and used as an anatomical landmark to assess the course of SN at this level. Indeed, the gluteus maximus muscle superficially, the quadratus femoris muscle deeply, and the proximal tendons of the hamstrings muscle complex - attaching to the distal portion of the ischial tuberosity - medially, define a virtual anatomical space holding the SN **(Figure 5A)**. Interestingly, the amount of fat tissue disposed in between the proximal tendons of the hamstrings muscle complex and the epifascicular epineurium of the SN is very small **(Video 1)**, and; in this sense, an abnormal tendons thickness due to pathological conditions - e.g., tendinosis, partial tear, calcifications - can lead to compression/irritation of the nearby peripheral nerve. [10] Moreover, excessive frictions involving the aforementioned histological interface can progressively lead to local inflammation phenomena and adhesions between the epineurium and epitenon with neural gliding impairment. [11] .

Gently shifting the probe more proximally along the ischial tuberosity, the proximal tendons of the hamstrings muscle complex progressively disappear to be replaced by the tendon of the quadratus

femoris muscle **(Figures 5B & C)**. At this level, in some patients, a “black bubble” can be identified in close proximity to the SN and erroneously misinterpreted as an edematous/swollen fascicle. The authors strongly suggest performing a color/power Doppler assessment of this sonographic finding because it is often related to a branch of the inferior gluteal artery known as *arteria comitans nervi ischiadici* **(Figures 5B & C)**. [12] Moreover, by minimizing the pressure of the probe over the skin, [13] the pulsation of the small arterial vessel can be easily identified promptly differentiating it from the surrounding hypoechoic fascicles of the SN **(Video 2)**.

Last but not least, ultrasound can be considered also a valuable diagnostic tool to assess eventual compression/entrapment of the SN secondary to occult fractures of the ischial tuberosity. In this sense, comparative scanning is paramount to differentiate cortical irregularities related to chronic mechanical enthesopathy of the proximal tendons of the hamstrings muscle complex from bony fractures. [14] Likewise, indirect sonographic signs of bone fractures such as subcutaneous edema - e.g., cobblestone pattern of the subcutis [13] - and periosteum abnormalities with/without local hematoma should be accurately checked as well. [14].

Ischiofemoral space

Fixing the medial edge of the probe over the ischial tuberosity and tilting its lateral edge towards the lesser trochanter of the femur **(Figure 6)**, the ischiofemoral space can be visualized **(Table 2)**. [15] At this level, dynamic sonographic scanning can be performed to observe in real-time how the ischiofemoral space changes its shape/dimension during the different motions and what happens to the anatomical structures located inside **(Video 3)**. [3]

Indeed, in patients with a clinical scenario suspected of ischiofemoral impingement, a peculiar sonographic finding has been described the pertinent literature. By (passively) externally rotating the hip until reaching the end-of-range motion, an abnormal/excessive bulging of the quadratus

femoris muscle belly which dislocates and compresses the SN against the ischial tuberosity has been observed reproducing the pain complained by the patient. [16] The latter has been defined as the "eruption" sign of quadratus femoris muscle, and coupled with the clinical findings should be considered among the multiple diagnostic tools to manage the complex clinical syndrome of the ischiofemoral impingement.

Of note, in patients with ultrasound assessment of the ischiofemoral space suggestive of dynamic pinching of the SN, we suggest accurately evaluating its echotexture for the eventual presence of swollen/edematous fascicles secondary to mechanical compression and damage of the neural microvasculature. [7]

Proximal thigh

Moving the probe distally to the ischial tuberosity in a transverse plane, the SN can be followed in the proximal third of the thigh located within the interfascial plane between the hamstrings muscle complex and adductor magnus muscle **(Video 4)**. Unlike the aforementioned anatomical regions presenting "hard" elements as bony prominences and large tendons; at this level, the nerve is mainly surrounded by "soft" tissues - muscles, fasciae - but several pathological conditions can lead to neural entrapment/irritation also at this level. For instance, a post-traumatic myofascial injury of the hamstrings complex **(Figure 7)** - exactly located in close proximity to the SN - can lead to compression and/or inflammation of the neural tissue due to the presence of hematoma in the acute phase or fibrotic tissue in the healing phase **(Video 5)**. Of note, a prompt sono-palpation of the aforementioned sonographic findings can be performed with the probe in an attempt to reproduce the pain usually complained by the patient. Indeed, if the local nociceptive pain can be related to the damaged myofascial tissue, the radiated neuropathic component may be associated with the irritation of the SN. [17] A strict clinical and sonographic follow-up is paramount to

guarantee a correct healing process of the myofascial injury avoiding local complications as perineural heterotopic ossifications **(Video 6)** and/or pseudocystic formations.

Last but not least, a dynamic scanning - in a longitudinal plane with isometric and/or isotonic contractions of the hamstrings complex - can be performed [10] during the healing phase to assess the eventual presence of adhesions in between the epifascicular epineurium of the SN and the fibrotic tissue of the scar **(Figure 8)**. [18] Unlike the physiological condition characterized by a differential gliding of the peripheral nerve with respect to the surrounding muscles, an en-block movement of the SN and the fibrotic scar can be observed in presence of a pathological adhesive interface.

PATHOLOGICAL CONDITIONS

In clinical practice, the deep gluteal syndrome is commonly used as an umbrella definition to refer to several pathological conditions characterized by non-discogenic entrapment of the SN in the subgluteal space. In this sense, we briefly describe the most common disorders involved in the aforementioned painful syndrome focusing on the practical aspects useful to guarantee an accurate sonographic examination of the SN and the surrounding anatomical structures in pathological conditions **(Table 3)**.

Piriformis syndrome

Hypertrophy of the piriformis muscle, anatomical variants of the SN and/or of the piriformis muscle, perineural fibrosis after open surgery, tendon avulsion, tendinosis, muscle strains, calcific tendinopathy, and muscle spasm are the most common causes of this syndrome. [4] Indeed, the authors suggest fully scrutinizing the piriformis muscle-tendon unit starting from its proximal muscular portion until its most distal tendinous component attaching to the bony surface of the greater trochanter. [19] Moreover, dynamic scanning with the patient prone should be performed

by matching hip internal rotation (i.e., stretching the piriformis muscle) and deep sono-palpation of the SN in an attempt to reproduce the symptoms complained by the patient due to its dynamic entrapment at this level **(Video 7)**. [3] Last but not least, a small fat pad is normally located in between the gluteus maximus muscle and piriformis muscle which should not be misinterpreted as fluid collection causing a secondary compression of the underlying SN. [18] Once again, dynamic scanning promptly shows the synchronized gliding movements of fat tissue and piriformis muscle during hip rotations confirming the exact diagnosis.

Gemelli-obturator internus complex syndrome

As previously mentioned in the scanning protocol, a scissor-like effect between the piriformis muscle and gemelli-obturator internus complex can be considered a (rare) cause of SN entrapment. Hypertrophy **(Figure 4)** and anatomical variants of the triceps coxae are usually described as the most common conditions leading to neural compression/irritation. [4] Based on the authors' experience, we suggest performing bilateral sono-palpation of the infrapiriform foramen in each and every patient to better distinguish normal vs. pathological sonographic findings in this very challenging anatomical site. Likewise, considering the difficulty in differentiating gemelli muscles from the obturator internus muscle we suggest using some technical tricks. Indeed, the presence of a hyperechoic intra-muscular tendon in the long-axis view; and, the "waterfall" moving pattern visible during the dynamic assessment - and related to the curved course of the obturator internus muscle wrapping the ischium **(Figure 3)** - allows prompt sonographic identification of this anatomical structure **(Figure 9)**. [15].

Ischiofemoral impingement syndrome

Excessive thickening of the quadratus femoris muscle can cause compression/rubbing of the SN within the ischiofemoral space. [4] In this sense, comparative sonographic scanning to measure

muscle thickness can be considered an essential step of the sonographic examination. Likewise, an intramuscular fluid collection - e.g., edema and/or hematoma - can be easily identified as a hypoechoic focus within the muscle belly. Interestingly, abnormal frictions at the muscle-nerve interface can progressively lead to perineural adhesions surrounding the epifascicular epineurium of the SN with impairment of the neural gliding during hip motions. [4].

Moreover, using the medial edge of the lesser trochanter and the lateral edge of the ischial tuberosity as bony landmarks, the size of ischiofemoral space can be measured to identify an eventual abnormal narrowing causing a mechanical impingement of soft tissues **(Figure 6)**. Indeed, the capability of US imaging for accurately measuring the dimension of ischiofemoral space was previously validated via magnetic resonance imaging in the pertinent literature. [20]

Hamstring syndrome

Proximal tendons of the hamstrings muscle complex can present a wide range of pathological conditions leading to an impingement with the nearby SN **(Figure 5)**. As previously mentioned in the scanning protocol, partial/complete tear, detachment, avulsion fracture, apophysitis of the ischial tuberosity, tendinosis, and calcific tendinopathy are the most common. [4] Dynamic entrapment of the SN secondary to pathological conditions involving the (proximal) tendon-bone complex of the hamstring muscles is also known as ischial tunnel syndrome. Of note, considering the peculiar spatial orientation of the bony surface of ischial tuberosity, a heel-toe maneuver is recommended redirecting the probe medially to optimize the simultaneous sonographic visualization of the tendons and SN. [10] Likewise, due to the different spatial course of the conjoint tendon of long head of the biceps femoris-semitendinosus and the semimembranosus tendon **(Figure 1C)**, a gentle tilting of the probe may be useful to avoid misinterpretation of anisotropy as a focal tendinosis at this level. [10] Last but not least, B-mode and color/power Doppler should be systematically coupled to assess the eventual presence of hypervascularization in between the epitenon of

proximal tendons of the hamstrings muscle complex and epifascicular epineurium of the SN; sonographic finding highly suggestive of perineural inflammatory phenomena. [7]

Others pathologies

Fibrous bands, gluteal contracture, and the impingement with orthopedic implants should also be considered as potential causes of non-discogenic entrapment of the SN. [4] Unlike the thin fibrotic strings which can be hardly visible using ultrasound; gluteal contracture, often presenting as sequelae of multiple intramuscular injections in the buttock, can be easily visualized. Indeed, it usually shows one or multiple hyperechoic fibrotic cords coupled with atrophic involution of the surrounding muscle tissue that can compress the SN along its subgluteal course. Lastly, sonographic tracking of the SN in close proximity of a metallic orthopedic hardware - e.g., hip prosthesis - can be easily performed to statically/dynamically assess an eventual impingement with compression and/or dislocation of the nerve. [21]

PITFALLS

In patients with a very high body mass index, thick subcutaneous fat tissue can significantly reduce the visibility of the SN [13], especially in its more proximal course within the buttock. In this sense, a low-frequency curvilinear probe could be necessary to identify the SN with a reduced spatial resolution of its echotexture. Likewise, chronic pathologies of the superficial lymphovascular network - e.g., lymphedema and lipedema - may lead to a fibrotic involution of the subcutis and/or dermis with a shielding effect of the deeper anatomical structures. [22 ; 23]. Reducing the frequency of ultrasound beam and accurately positioning the focus at the level of the SN can be considered simple technical adjustments to optimize its visualization in these cases.

Last but not least, in older patients, sarcopenia – which mainly involves the lower limb muscles - can progress from muscle mass loss to fibrofatty involution of the muscle tissue. [24] Once again,

multiple “pathological” acoustic interfaces that attenuate the ultrasonic beam [25] worse the visibility of the SN located deep to the misty muscles. [26]

Acknowledgements

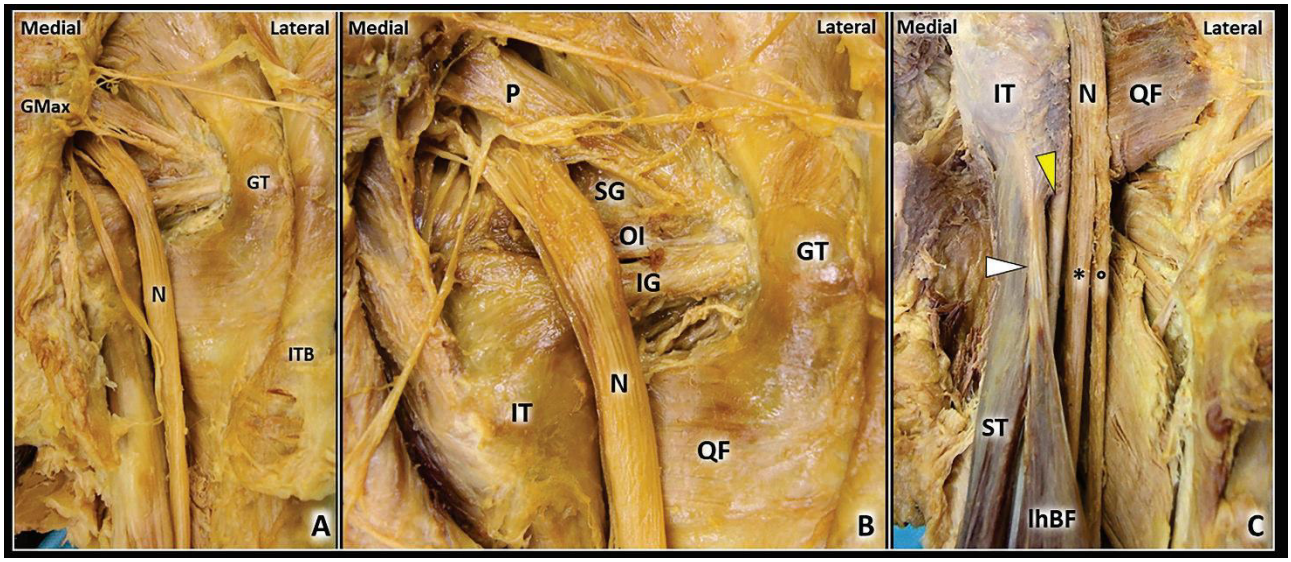
The pictures of the anatomic specimens were elaborated using donated bodies with the approval of the Institute of Anatomy, First Faculty of Medicine, Charles University, Prague.

The authors sincerely thank those who donated their bodies to science so that anatomical research could be performed. Results from such research can potentially increase mankind’s overall knowledge that would improve patient care. Therefore, these donors and their families deserve our highest gratitude.

Figure legends

Figure 1

Cadaveric anatomy of the sciatic nerve.



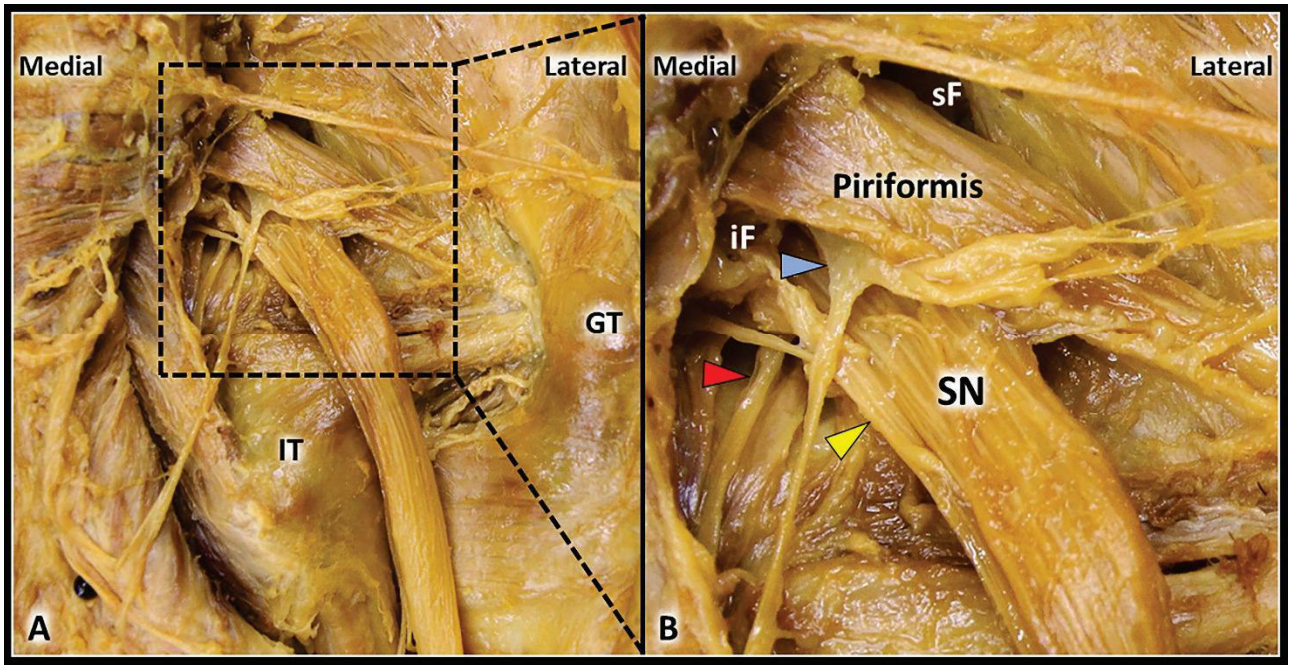
Cutting and lifting the gluteus maximus *(GMax)*-iliotibial band *(ITB)* complex, the sciatic nerve *(N)* can be promptly visualized in the cadaveric specimen **(A)**. Crossed the infrapiriform foramen the sciatic nerve *(N)* runs over the superior gemellus *(SG)*, obturator internus *(OI)* and inferior gemellus *(IG)* muscles – the *triceps coxae*; then, it slips over the quadratus femoris muscle *(QF)* laterally to

the ischial tuberosity *(IT)* **(B)**. More caudally, the sciatic nerve *(N)* reaches the posterior compartment of the thigh **(C)**, below the long head of the biceps femoris muscle *(lhBF)*, and laterally to the semimembranosus tendon *(yellow arrowhead)* and semitendinosus muscle *(ST)*. Interestingly, in this cadaveric specimen, the sciatic nerve *(N)* splits very proximally in the tibial nerve *(black asterisk)* and the common peroneal nerve *(black dot)*.

GT: greater trochanter, P: piriformis muscle, white arrowhead: conjoint tendon of long head of the biceps femoris-semitendinosus

Figure 2

Cadaveric anatomy of the infrapiriform foramen.

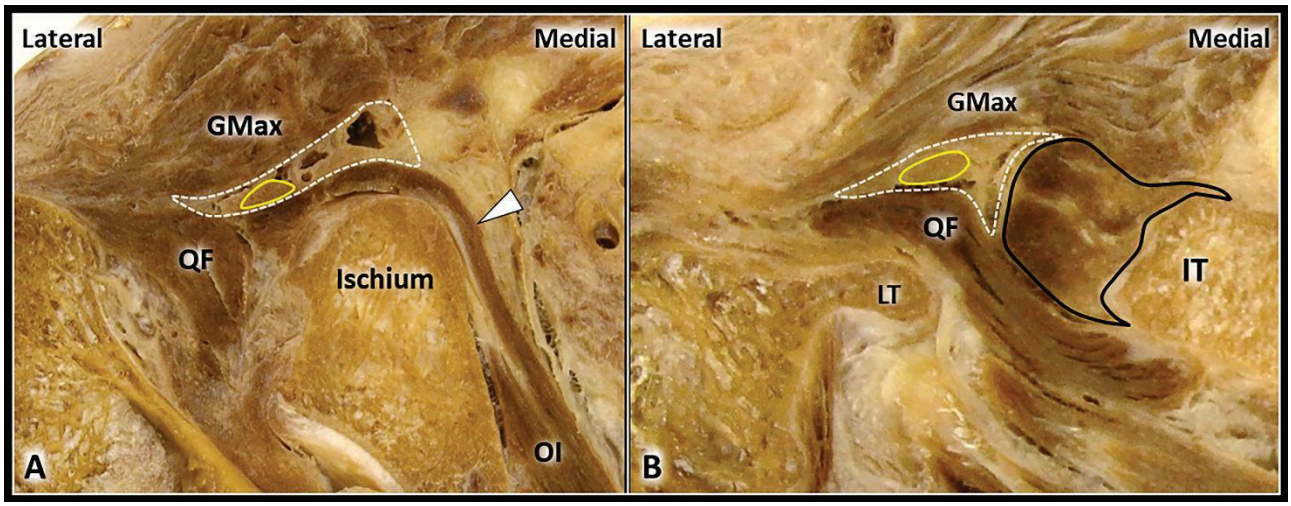


Magnification of the greater sciatic foramen **(A, B)** shows the inferior gluteal veins *(light blue arrowhead)*, the internal pudendal artery *(red arrowhead)*, the posterior femoral cutaneous nerve *(yellow arrowhead)*, and the sciatic nerve *(SN)* while crossing the infrapiriformis foramen *(iF)*.

sF: suprapiriform foramen, GT: greater trochanter, IT: ischial tuberosity

Figure 3

Cadaveric anatomy of the deep gluteal space.

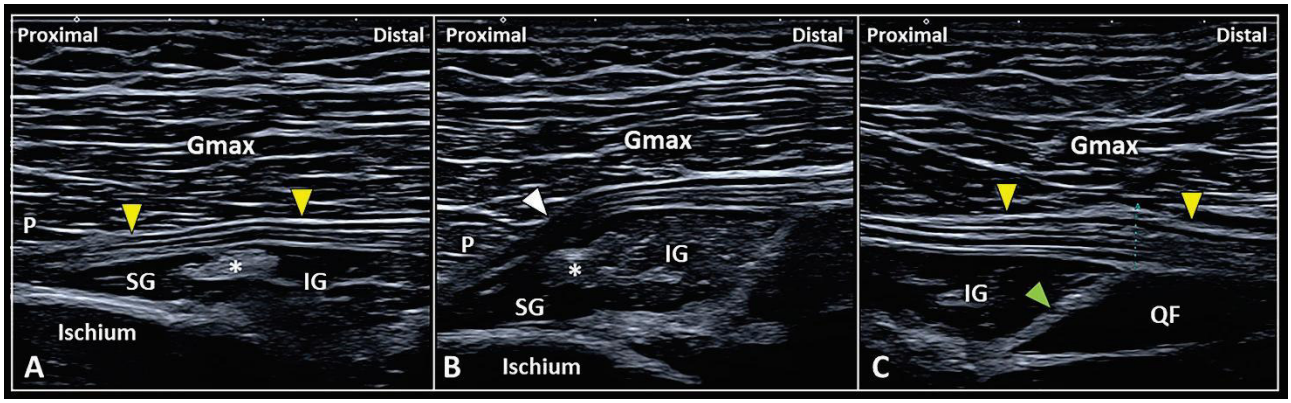


The deep gluteal space *(white dotted line)* is a virtual space located under the gluteus maximus muscle *(Gmax)* and filled with fat tissue, nerves, and vascular elements. In the cadaveric slices the obturator internus muscle *(OI)* proximally **(A)**, and the quadratus femoris muscle *(QF)* coupled with the proximal tendons of the hamstrings muscle complex *(black line)* distally **(B)**, define its deep edges. It is interesting to observe how the thin extension *(white arrowhead)* of the obturator internus muscle *(OI)* wraps the bony surface of the ischium in an anterior-to-posterior fashion interposing between the sciatic nerve *(yellow line)* and the bony cortex like a muscula "cushion" **(A)**.

IT: ischial tuberosity, LT: lesser trochanter

Figure 4

Ultrasound imaging of the infrapiriform foramen.

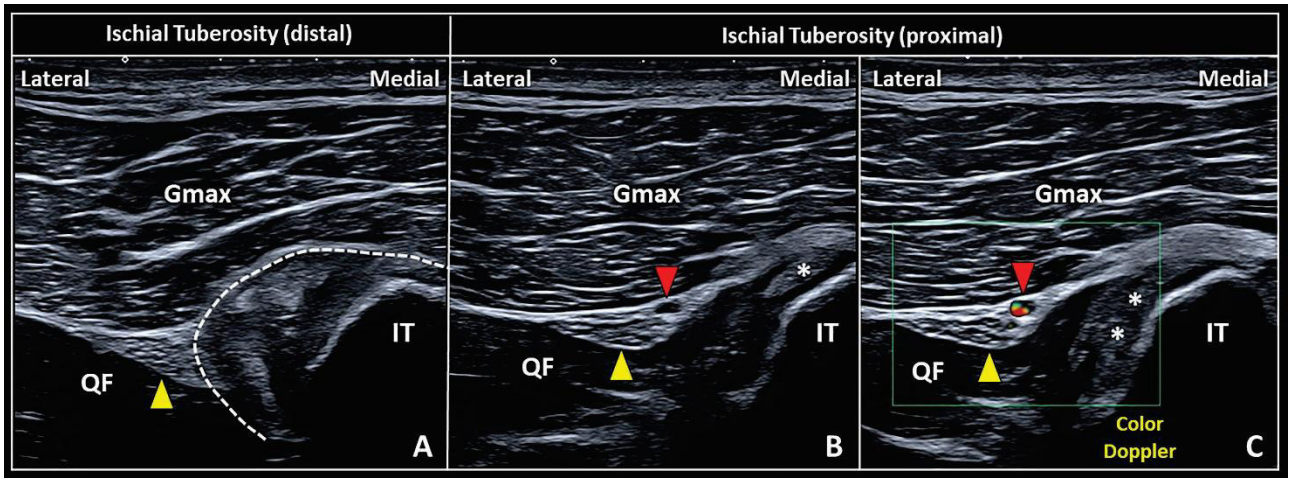


Normally, the sciatic nerve *(yellow arrowheads)* presents a regular fascicular texture and gently emerges from the inferior edge of the piriformis muscle *(P)* to slip over the gemelli-obturator internus complex **(A)**. In some patients, hypertrophy of the inferior gemellus *(IG)* forces the sciatic nerve to make a sharp bend *(white arrowhead)* to exit the infrapiriform foramen – i.e., the so-called dive sign **(B)**. More distally, a hyperechoic connective septum *(green arrowhead)* clearly defines the histological interface between the inferior gemellus *(IG)* and quadratus femoris *(QF)* muscles **(C)**.

Gmax: gluteus maximus muscle, SG: superior gemellus, white asterisk: obturator internus tendon

Figure 5

Ultrasound imaging of the ischial tuberosity region.



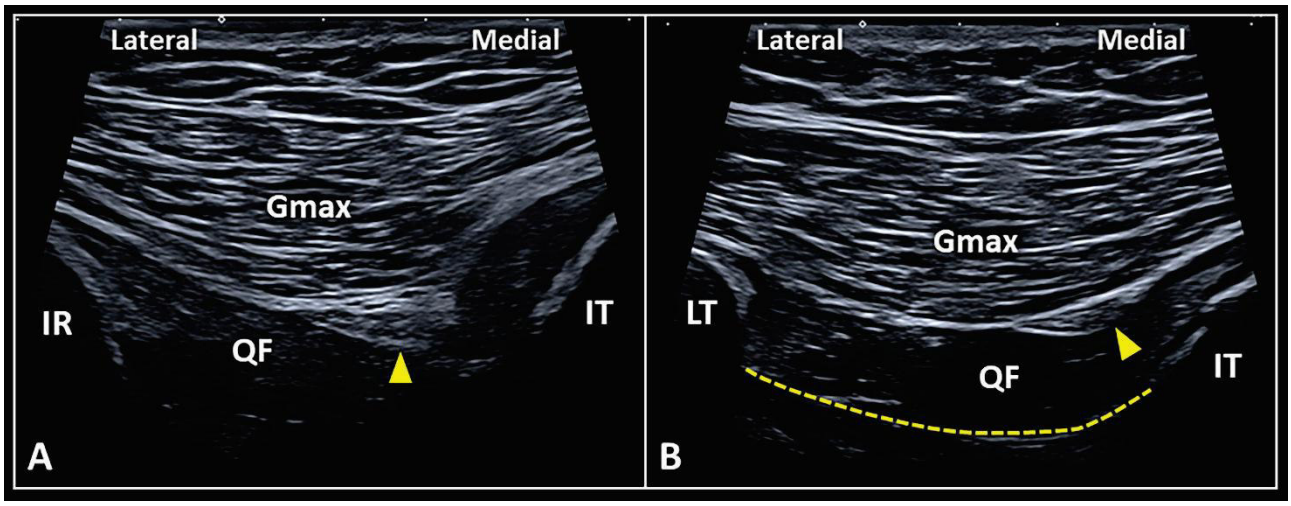
Using a transverse scan over the distal portion of the ischial tuberosity *(IT)*, the contact interface between the sciatic nerve *(yellow arrowhead)* and the proximal tendons of the hamstrings muscle complex *(white dotted line)* is clearly visible **(A)**. Shifting the probe proximally at the level of the

quadratus femoris tendon *(white asterisks)*, in some patients a small branch of the inferior gluteal artery *(red arrowhead)* can be identified accompanying the sciatic nerve *(yellow arrowhead)* which should not be misinterpreted as a nerve fascicle **(B, C)**.

Gmax: gluteus maximus muscle, QF: quadratus femoris muscle, CD: color doppler

Figure 6

Ultrasound imaging of the ischiofemoral space

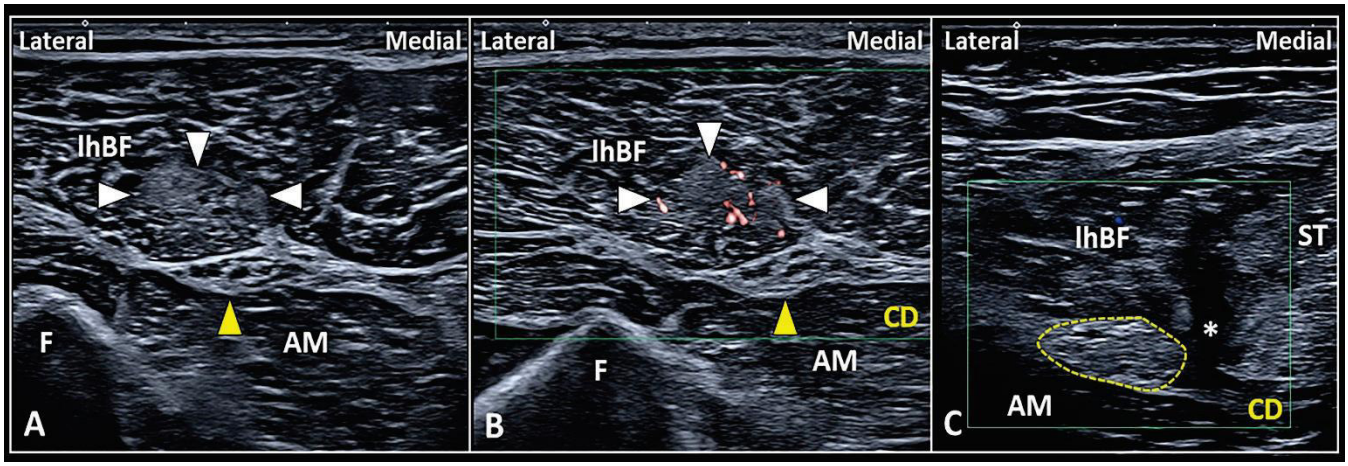


Starting with the probe in a transverse position **(A)** the ischial tuberosity *(IT)* and the intertrocantheric ridge *(IR)* can be used as bony landmarks; than, gently aligning the probe in the long-axis view of quadratus femoris muscle *(QF)*, the lesser trochanter *(LT)* clearly define the lateral edge of ischiofemoral space *(yellow dotted line)*.

Gmax: gluteus maximus muscle, yellow arrowhead: sciatic nerve

Figure 7

Ultrasound imaging of the proximal thigh.

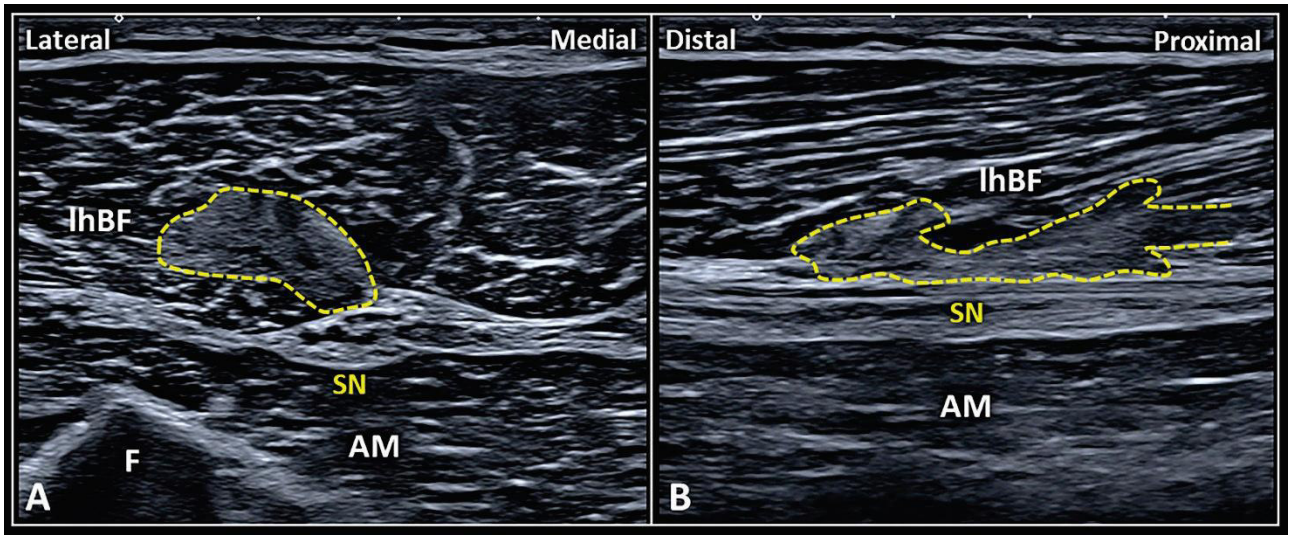


B-mode **(A)** and color Doppler **(B)** scans clearly show a focus of granulation tissue *(white arrowheads)* located in the deep portion of the long head of the biceps femoris *(lhBF)* which mechanically compresses the underlying sciatic nerve *(yellow arrowhead)*. Of note, the intralesional vascular signals are highly suggestive of an "immature" scar not ready for a maximal load **(B)**. Likewise, in the acute phase of trauma **(C)**, the hematoma/edema *(white asterisk)* can reach the epifascicular epineurium *(yellow dotted line)* of the sciatic nerve increasing the perineural pressure and evoking neuropathic pain.

CD: color doppler, AM: adductor magnus muscle, ST: semitendinosus muscle, F: femur

Figure 8

Ultrasound imaging of the sciatic nerve-scar tissue interface.

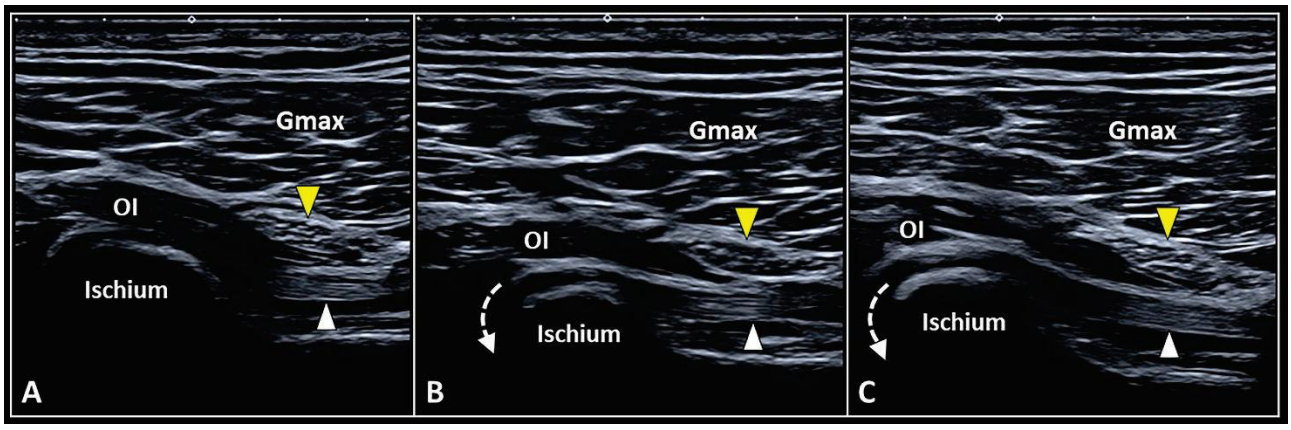


Starting from a transverse scan **(A)**, the medial portion of the fibrous tissue *(yellow dotted line)* is clearly visible in direct contact with the underlying epifascicular epineurium of the sciatic nerve *(SN)*. Rotating the probe 90 degrees in a longitudinal plane **(B)**, dynamic scanning can be performed to assess how the sciatic nerve *(SN)* and the surrounding scar tissue *(yellow dotted line)* interact with each other.

AM: adductor magnus muscle, F: femur, lhBF: long head of the biceps femoris muscle

Figure 9

Ultrasound imaging of the obturator internus muscle.



Starting from a transverse oblique scan the obturator internus muscle *(OI)* can be visualized covering the ischium like a hood **(A)**. An external rotation of the hip **(B, C)** can be performed to promptly

observe the waterfall movement *(curved dotted arrow)* of the muscle belly slipping deeply, and the dynamic gliding of the intramuscular tendon *(white arrowhead)* underlying the sciatic nerve *(yellow arrowhead)*. Gmax: gluteus maximus muscle

Video legends

Video 1

Proximal-to-distal sonotracking of the SN promptly shows a very small amount (almost absent) of fat tissue within the histological interface between the epifascicular epineurium and the epitenon of the proximal hamstrings tendon.



Video 1.avi

Video 2

The pulsation of arteria comitans nervi ischiadici is easily visible reducing the pressure of the ultrasound probe over the skin of the patient. Using this simple technical trick it can be easily differentiated from the fascicles of the SN.



Video 2.avi

Video 3

Dynamic ultrasound assessment of the ischiofemoral space shows a regular gliding of the quadratus femoris muscle without pinching fenomena of the schiatic nerve located in proximity of the ischial tuberosity.



Video 3.avi

Video 4

Sonotracking of the sciatic nerve at the proximal third of the thigh clearly shows its anatomical course within a “soft case” composed of the hamstrings muscle and adductor magnus muscle.



Video 4.avi

Video 5

Vascular signals within the granulation tissue are often related to a still active healing process with an “immature” scar. In this sense, it can be considered a very useful sonographic sign to accurately manage the load and training.



Video 5.avi

Video 6

Longitudinal sonographic scan of the sciatic nerve shows a perineural calcification with a complete acoustic shadow at the proximal third of the thigh.



Video 6.avi

Video 7

A “pear-shaped” muscle can be easily observed coming out from the greater sciatic foramen and gliding in between the gluteus maximus muscle and the SN during internal hip rotation.



Video 7.avi

Table 1. Greater sciatic foramen.

Boundaries	*Superior*: anterior sacroiliac ligament *Posteromedial*: sacrotuberous ligament *Inferior*: sacrospinous ligament and ischial spine *Anterolateral*: greater sciatic notch
Nerves	***Suprapiriform foramen***: superior gluteal nerve ***Infrapiriform foramen***: sciatic nerve, inferior gluteal nerve, pudendal nerve, nerve to obturator internus, nerve to quadratus femoris, posterior femoral cutaneous nerv (n. cutaneus femoris dorsalis) §
Vessels	***Suprapiriform foramen***: superior gluteal vessels ***Infrapiriform foramen***: inferior gluteal vessels, internal pudendal vessels

§ posterior femoral cutaneous nerve can be merged with the inferior gluteal nerve defining a unique peripheral nerve known as *minor sciatic nerve* (Obach 1983)

Table 2. Ischiofemoral space.

Superior	Femoral neck, ischiofemoral ligament, inferior gemellus muscle
Inferior	Inferior edge of quadratus femoris muscle
Medial	Ischial tuberosity
Lateral	Lesser trochanter of the femur, intertrochanteric crest of the femur

Table 3. Dynamic ultrasound for deep gluteal syndrome.

Pathology	Dynamic maneuvers
Piriformis syndrome	Internal hip rotation (stretching the piriformis muscle) with simultaneous sonopalpation of the SN

Gemelli-obturator internus complex syndrome	Isometric contraction of the triceps coxae or internal hip rotation [(1)]
Ischiofemoral impingement syndrome	External hip rotation [(2)]
Hamstring syndrome	Sono-compression of the SN against the proximal tendons of hamstrings muscle complex [(3)]

(1) symptomatic/asymptomatic scissor-like effect of the infrapiriform foramen
(2) eruption sign, dynamic pinching of the SN in between the ischial tuberosity and quadratus femoris
(3) sono-Tinel of the SN at the ischial tunnel

References

1. Dupont G, Unno F, Iwanaga J, et al. A variant of the sciatic nerve and its clinical implications. Cureus. 2018; 10(6): e2874. doi: 10.7759/cureus.2874.
2. Giuffre BA, Jeanmonod R. Anatomy, Sciatic Nerve. 2022 Jul 25. In: StatPearls [Internet]. Treasure Island (FL): StatPearls Publishing; 2022 Jan–. PMID: 29494038.
3. Mezian K, Ricci V, Güvener O, et al. EURO-MUSCULUS/USPRM dynamic ultrasound protocols for (adult) hip. Am J Phys Med Rehabil. 2022; 101(11): e162-e168. doi: 10.1097/PHM.0000000000002061.
4. Hernando MF, Cerezal L, Pérez-Carro L, et al. Deep gluteal syndrome: anatomy, imaging, and management of sciatic nerve entrapments in the subgluteal space. Skeletal Radiol. 2015; 44(7): 919-34. doi: 10.1007/s00256-015-2124-6.
5. Pérez-Carro L, Fernandez-Hernando M, Cerezal L, et al. Deep gluteal space problems: piriformis syndrome, ischiofemoral impingement and sciatic nerve release. Muscles Ligaments Tendons J. 2016; 21: 384–96. doi: 10.11138/mltj/2016.6.3.384.
6. Balius R, Susín A, Morros C, et al. Gemelli-obturator complex in the deep gluteal space: an anatomic and dynamic study. Skeletal Radiol. 2018; 47(6): 763-770. doi: 10.1007/s00256-017-2831-2.

7. Ricci V, Ricci C, Cocco G, et al. Histopathology and high-resolution ultrasound imaging for peripheral nerve (injuries). J Neurol. 2022; 269(7): 3663-3675. doi: 10.1007/s00415-022-10988-1.
8. Kanawati AJ. Variations of the sciatic nerve anatomy and blood supply in the gluteal region: a review of the literature. ANZ J Surg. 2014; 84(11): 816-9. doi: 10.1111/ans.12675.
9. Balius R, Pujol M, Pérez-Cuenca D, et al. Sciatic nerve movement in the deep gluteal space during hip rotations maneuvers. Clin Anat. 2022; 35(4): 482-491. doi: 10.1002/ca.23828.
10. Becciolini M, Bonacchi G, Bianchi S. Ultrasound features of the proximal hamstring muscle-tendon-bone unit. J Ultrasound Med. 2019; 38(5): 1367-1382. doi: 10.1002/jum.14804.
11. Chang KV, Wu WT, Özçakar L. Ultrasound imaging and guidance in peripheral nerve entrapment: hydrodissection highlighted. Pain Manag. 2020; 10(2): 97-106. doi: 10.2217/pmt-2019-0056.
12. Ishizawa A, Hayashi S, Nasu H, et al. An artery accompanying the sciatic nerve (arteria comitans nervi ischiadici) and the position of the hip joint: a comparative histological study using chick, mouse, and human foetal specimens. Folia Morphol (Warsz). 2013; 72(1): 41-50. doi: 10.5603/fm.2013.0007.
13. Ricci V, Ricci C, Cocco G, et al. From histology to sonography in skin and superficial tissue disorders: EURO-MUSCULUS/USPRM* approach. Pathol Res Pract. 2022; 237: 154003. doi: 10.1016/j.prp.2022.154003.
14. Cocco G, Ricci V, Villani M, et al. Ultrasound imaging of bone fractures. Insights Imaging. 2022; 13(1): 189. doi: 10.1186/s13244-022-01335-z.
15. Wu WT, Chang KV, Mezian K, Naňka O, Ricci V, Chang HC, Wang B, Hung CY, Özçakar L. Ischiofemoral Impingement Syndrome: Clinical and Imaging/Guidance Issues with Special

Focus on Ultrasonography. Diagnostics (Basel). 2022 Dec 31;13(1):139. doi: 10.3390/diagnostics13010139. PMID: 36611431.

16. Chen YT, Jenkins KM. Ultrasound finding of ischiofemoral impingement syndrome and novel treatment with botulinum toxin chemodenervation: a case report. PM R. 2018; 10(6): 665-670. doi: 10.1016/j.pmrj.2017.11.010.
17. Ricci V, Ricci C, Gervasoni F, et al. From histoanatomy to sonography in myofascial pain syndrome: a EURO-MUSCULUS/USPRM approach. Am J Phys Med Rehabil. 2023; 102(1): 92-97. doi: 10.1097/PHM.0000000000001975.
18. Chang KV, Wu WT, Mezian K, Naňka O, Özçakar L. Letter to the Editor Regarding "Feasibility and Reliability of an Ultrasound Examination to Diagnose Piriformis Syndrome". World Neurosurg. 2020; 137: 483-484.
19. Chang KV, Wu WT, Lew HL, Özçakar L. Ultrasound Imaging and Guided Injection for the Lateral and Posterior Hip. Am J Phys Med Rehabil. 2018 Apr;97(4):285-291. doi: 10.1097/PHM.0000000000000895. PMID: 29324458.
20. Finnoff JT, Johnson AC, Hollman JH. Can Ultrasound Accurately Assess Ischiofemoral Space Dimensions? A Validation Study. PM R. 2017 Apr;9(4):392-397. doi: 10.1016/j.pmrj.2016.06.024. Epub 2016 Jul 12. PMID: 27418573.
21. Guillin R, Botchu R, Bianchi S. Sonography of orthopedic hardware impingement of the extremities. J Ultrasound Med. 2012 Sep;31(9):1457-63. doi: 10.7863/jum.2012.31.9.1457. PMID: 22922627.
22. Ricci V, Ricci C, Gervasoni F, et al. From histo-anatomy to sonography in lymphedema: EURO-MUSCULUS/USPRM approach. Eur J Phys Rehabil Med. 2022; 58(1): 108-117. doi: 10.23736/S1973-9087.21.06853-2.

23. Ricci V, Ricci C, Gervasoni F, et al. From physical to ultrasound examination in lymphedema: a novel dynamic approach. J Ultrasound. 2022; 25(3): 757-763. doi: 10.1007/s40477-021-00633-4.
24. Kara M, Kaymak B, Frontera W, et al. Diagnosing sarcopenia: functional perspectives and a new algorithm from the ISarcoPRM. J Rehabil Med. 2021; 53(6): jrm00209. doi: 10.2340/16501977-2851.
25. Ricci V, Soylu AR, Özçakar L. Artifacts and artistic facts: a visual simulation for ultrasound training. Am J Phys Med Rehabil. 2019; 98(6): 521-525. doi: 10.1097/PHM.0000000000001134.
26. Jačisko J, Ricci V, Mezian K, et al. Mnemonics and metaphorical videos for detecting/diagnosing musculoskeletal sonopathologies. Am J Phys Med Rehabil. 2022 Oct 11. doi: 10.1097/PHM.0000000000002119. Epub ahead of print. PMID: 36228196.

2.2 Dynamic Ultrasound Assessment for Insertional Achilles Tendinopathy: the CORI (Cocco-Ricci) Sign

Abstract

Objective

To describe a novel, dynamic ultrasound assessment of the Achilles tendon at the calcaneal insertion taking advantage of the effusion within the deep retrocalcaneal bursa as a natural contrast agent.

Materials and Methods

Positioning the ultrasound transducer in a longitudinal plane over the Achilles tendon at the calcaneal insertion, manual compression of the deep retrocalcaneal bursa can be performed

using the other hand. Dynamically shifting the anechoic effusion from the proximal to the distal compartment of the bursa, the deep surface of the Achilles tendon is lifted from the underlying cortical bone of the posterosuperior tuberosity of the calcaneus.

Results

Pushing the anechoic effusion from the bursal cavity toward the undersurface of the Achilles tendon, an eventual focal injury of its deep fibers can be promptly visualized dynamically during the maneuver as a “black crescent” within the tendon - i.e., the CORI (Cocco-Ricci) sign.

Conclusion

The CORI sign is a novel sonographic sign to further enhance the diagnostic accuracy of dynamic ultrasound imaging in patients with insertional Achilles tendinopathy especially to detect focal injury involving the deep fibers of the tendon.

Abbreviations

AT: Achilles tendon, IAT: insertional Achilles tendinopathy, DRB: deep retrocalcaneal bursa, US: ultrasound

Introduction

Pain and swelling at the calcaneal attachment of the Achilles tendon (AT) define the clinical scenario of insertional Achilles tendinopathy (IAT). [1, 2] The distal portion of the AT, the (cartilaginous) tendon-bone junction, the deep retrocalcaneal bursa (DRB), and the subcutaneous calcaneal bursa are the pain generators commonly involved in the IAT. [1-3] The DRB is a V-shaped virtual cavity presenting fibrocartilaginous and synovial walls interposed between the posteroinferior wedge of the Kager’s fat pad, the posterior surface

of the calcaneus, and the AT. [3] It presents a mean overall volume of 1.0-1.5 mL with a distal tip between the AT and the calcaneus posterosuperior tuberosity; and, a proximal bifurcation protruding within the Kager's fat tissue with a posterior and anterior recess. [4] Bursal effusion and synovial hypertrophy are the most common pathological sonographic signs involving this anatomical structure in IAT patients. [4]

Previous standardized dynamic ultrasound (US) protocols have been published in the pertinent literature to assess the hindfoot during active and passive ankle movements. [5] Likewise, the undersurface of AT at its course over the posterosuperior tuberosity of the calcaneus remains a very challenging anatomical site to evaluate with the US making the diagnosis of focal injury involving the deep tendon fibers a potential pitfall especially for novice sonographers. In this sense, the present technical report proposes a novel dynamic maneuver to “pump” the bursal effusion between the cortical bone of the calcaneus and the undersurface of AT accurately assessing its deep fibers. The novel sign introduced in this report is called the CORI (Cocco-Ricci) sign, reflecting the collaborative effort and contributions of the researchers Cocco and Ricci.

Materials and Methods

The authors defined three progressive steps in the present technical report to perform a comprehensive sonographic assessment of deep retrocalcaneal space in IAT patients describing the novel dynamic maneuver and the CORI sign – i.e., patient and transducer positioning, and static and dynamic ultrasound examination.

Patient and Transducer Positioning

The patient is prone with the ankle joint in a neutral position and the foot hanging over the edge of the examination bed **(Figure 1)**. A large amount of gel must be positioned between

the ultrasound transducer and the heel skin to avoid an unintentional compression of the superficial soft tissues of the posterior calcaneus preserving the native shape of the different histological layers. [6] The ultrasound transducer is positioned in a longitudinal plane, covering the distal portion of the AT and the entire posterior surface of the heel. A linear, high-frequency transducer must be adopted to guarantee high spatial resolution sonographic images of the retrocalcaneal space.

Static Ultrasound Examination

The dermo-epidermal complex, the AT, the Kager's fat pad, the DRB, and the posterior calcaneus are visualized during static ultrasound assessment. Thickening of the subcutaneous tissue related to fibrotic involution of the fat tissue or hypertrophy of the subcutaneous calcaneal bursa (pre Achilles bursa) may be observed superficially to the AT. [6, 7] Bony spurs, bone pitting, and cortical bone erosions are the most common sonographic findings at the tendon-bone junction. [7, 8] Tendinosis with hypoechoic thickening of the tendon tissue and disappearance of the fibrillar pattern, intra-tendinous calcification/bone formation with acoustic shadow, and focal injury must be accurately checked along the distal portion of the AT wrapping the calcaneal posterior surface. Of note, the latter presents a posterosuperior tuberosity covered by fibrocartilage (i.s., the periosteal fibrocartilage) and a posterior facet that represents the footprint of the AT. [3] Indeed, the AT runs over the posterosuperior tuberosity and attaches to the posterior bony facet of the calcaneus. [9, 10] Lastly, anechoic bursal effusion with/without hypoechoic synovial hypertrophy and focal hyperechogenicity of the posteroinferior wedge of Kager's fat pad due to edema are the sonographic signs involving the deep retrocalcaneal space in IAT patients. [7]

Considering the prone position of the patient and the anatomical architecture of the DRB, effusion commonly collects inside the anterior and posterior bursal recess (proximal

compartment of the bursa) but not within its distal tip. In this sense, the AT is usually "squeezed" over the periosteal fibrocartilage of the posterosuperior tuberosity of the calcaneus, making the diagnosis of focal deep fibers disruption very challenging.

Dynamic Ultrasound Examination

In IAT patients with effusion of the DRB, a dynamic maneuver can be performed to optimize the assessment of the AT-posterosuperior tuberosity interface. Holding the transducer over the posterior surface of the heel with a large amount of gel (i.e., the stand-off technique), the other hand can be used to squeeze the deep retrocalcaneal space **(Figure 1, Video 1)**. Intermittent compression of soft tissues located between the AT and the calcaneus promptly shifts the bursal effusion from its anterior/posterior recess towards the distal tip. The patient must be asked to leave the foot completely free during the dynamic maneuver.

Results

In patients with focal disruption of deep fibers of AT, manual compression of the deep retrocalcaneal space leads the (anechoic) bursal effusion to migrate inside the tendon injury opening the pathological gap and generating a "black crescent" called the CORI sign **(Video 2)**. Of note, the fluid acts as a natural contrast agent migrating from the anterior/posterior recess to the distal tip of the bursa revealing the proximal stump of injured tendon fibers **(Figure 2)**. Releasing the manual compression over the retrocalcaneal space of the heel, anechoic effusion flows back toward the posteroinferior wedge of the Kager's fat pad distending the large proximal recesses of the DRB (anterior and posterior recess of the bursa).

Discussion

The IAT is a common disorder of the hindfoot involving the bone tissue of the calcaneus and surrounding soft tissues. [1, 2] The X-ray for the bones and the US for the soft tissues are the first-line imaging modalities usually performed in clinical practice to optimize the management of this painful condition. [1, 2] Among the different anatomical structures of the retrocalcaneal space, the AT-posterosuperior tuberosity interface is one of the most challenging to assess using static ultrasound. Indeed, the prone position of the patient with the foot hanging over the edge of the examination bed “closes” the tendon-bone interface making the sonographic visualization of effusion or tendon disruption at this level not easy, especially for beginners.

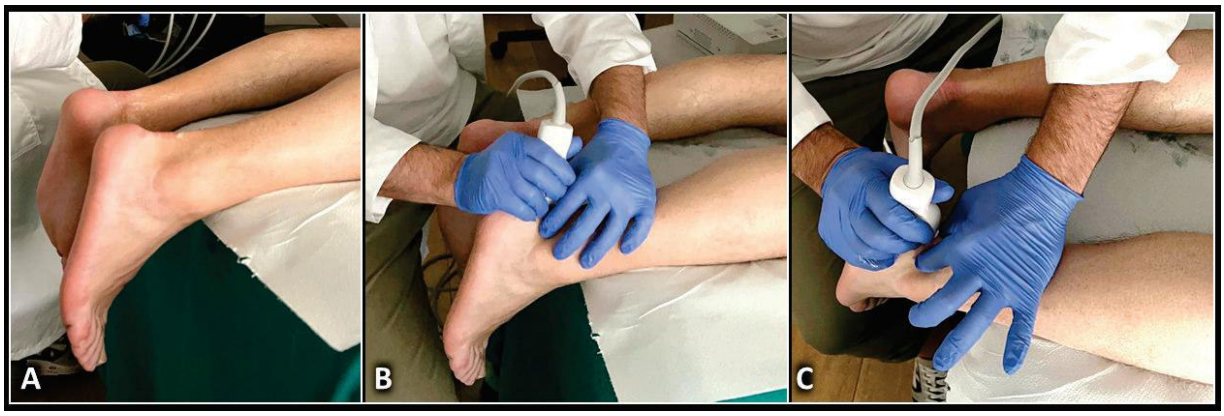
Static US examination commonly presents a combination of anechoic effusion inside the anterior/posterior recess of DRB and hypervascularization of deep fibers of AT at the anatomical passage over the posterosuperior tuberosity of the calcaneus **(Video 3)**. Hyperemia of the AT undersurface may be considered a static sonographic sign suggestive of a potential focal injury of deep fibers and require an adjunctive dynamic assessment using the manual compression of the DRB. Indeed, pushing the bursal effusion inside its distal tip the anechoic fluid may promptly fill the tendon gap showing the “black crescent” called the CORI sign **(Video 2)**. Lastly, the sonographic tracking of the AT from proximal to distal and vice versa must be performed to confirm the tendon injury in a transverse plane **(Figure 3, Video 4)**.

Conclusion

Dynamic ultrasound assessment of the hindfoot by manually squeezing the deep retrocalcaneal space and the CORI sign can be considered novel diagnostic tools to optimize the diagnosis of “hidden” tendon injury involving the undersurface of AT in IAT patients.

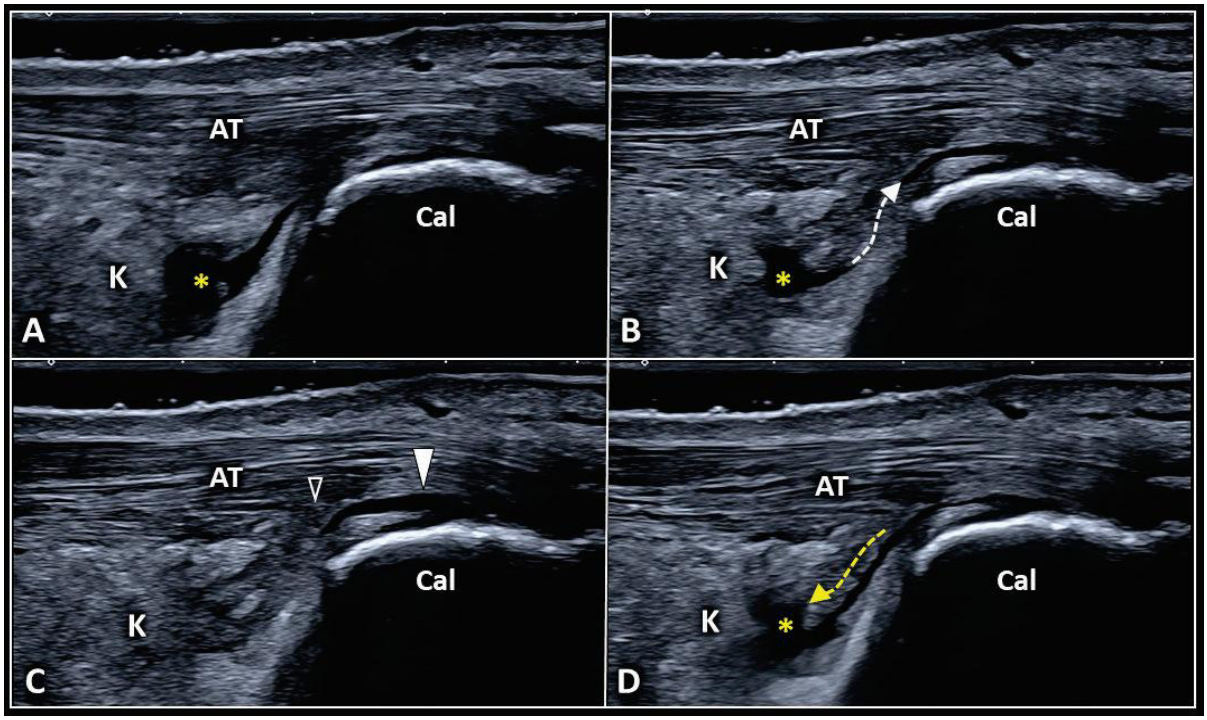
Figure Legends

Figure 1. Patient/transducer positioning and dynamic maneuver.



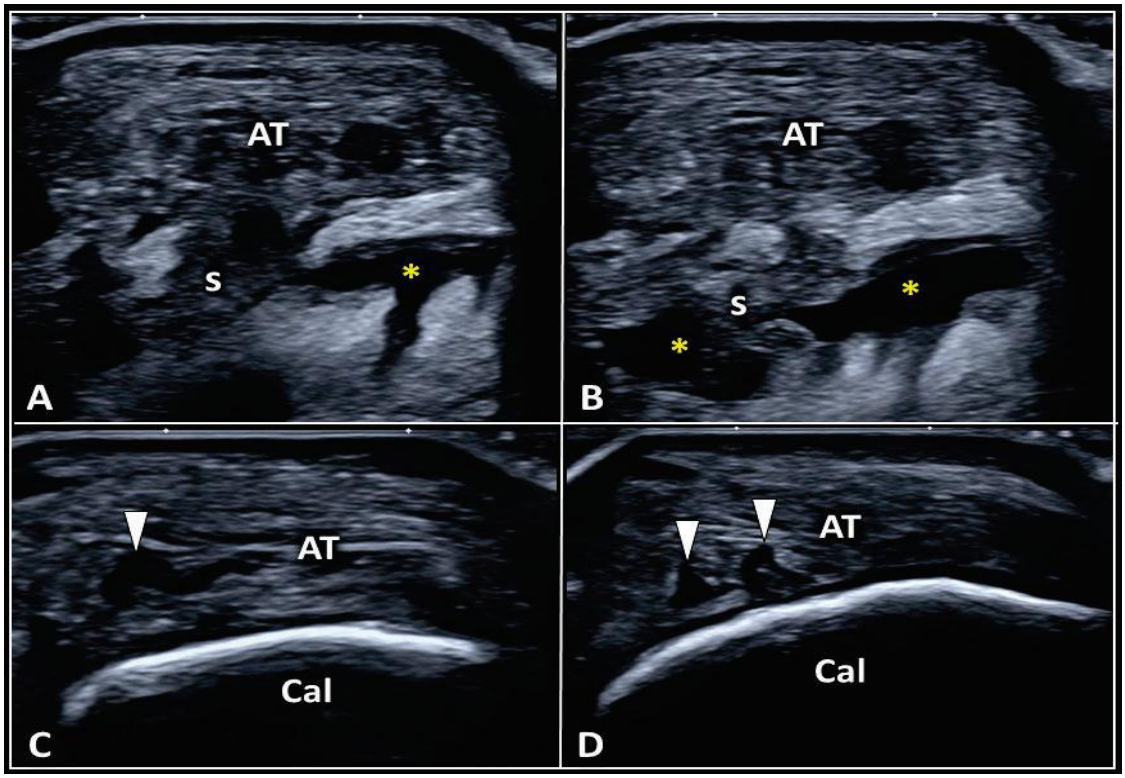
With the patient in a prone position and the foot hanging over the edge of the examination bed **(A)**, the ultrasound transducer is positioned in a longitudinal plane over the posterior aspect of the heel **(B)**, and the manual compression of deep retrocalcaneal space is performed with the other hand **(C)**.

Figure 2. Dynamic ultrasound assessment of the deep retrocalcaneal space and CORI sign.



Starting from a static condition **(A)** with anechoic effusion *(yellow asterisk)* inside the proximal compartment of the DRB, a manual squeezing of the retrocalcaneal space is performed pushing the fluid *(white dotted arrow)* within the distal compartment of the synovial bursa **(B)**. Using this technique, the fluid acts as a natural contrast agent dilating the AT-posterosuperior tuberosity interface and promptly visualizing a "black crescent" *(white arrowhead)* within the focal disruption of deep fibers of the tendon **(C)**. Releasing the manual compression of the hindfoot *(D)*, the anechoic effusion *(yellow asterisk)* progressively flows back *(yellow dotted arrow)* inside the proximal and anterior synovial recess of the DRB. AT: Achilles tendon, K: Kager's fat pad, Cal: calcaneus, void arrowhead: proximal stump of disrupted tendon fibers

Figure 3. Sonographic tracking of AT in a transverse plane.



Starting proximally **(A, B)** and progressively shifting the transducer distally **(C, D)**, the bursal effusion *(yellow asterisk)*, synovial hypertrophy *(s)*, and focal disruption of deep fibers *(white arrowheads)* of AT have been confirmed in a short axis view. AT: Achilles tendon, Cal: calcaneus

Video Legends

Video 1. Patient/transducer positioning and dynamic maneuver.

Video 1.avi

Video 2. Manual compression of deep retrocalcaneal space promptly shifts the anechoic fluid from the anterior recess of the bursa to its distal tip “opening” the injury of the AT undersurface and showing the “black crescent” called the CORI sign.

Video 2.avi

Video 3. Static ultrasound imaging shows the anechoic fluid inside the anterior recess of the DRB and the hypervascularization involving the deep fibers of the tendon at the AT-posterosuperior tuberosity interface.

Video 3.avi

Video 4. Sonographic tracking of the AT in a transverse plan to confirm the disruption of deep fibers of AT at the calcaneal attachment.



Video 4.avi

References

1. Krishna Sayana M, Maffulli N. Insertional achilles tendinopathy. *Foot Ankle Clin*. 2005; 10(2): 309-20. doi: 10.1016/j.fcl.2005.01.010.
2. van Dijk CN, van Sterkenburg MN, Wiegerinck JI, Karlsson J, Maffulli N. Terminology for achilles tendon related disorders. *Knee Surg Sports Traumatol Arthrosc*. 2011; 19(5): 835-41. doi: 10.1007/s00167-010-1374-z.
3. Shaw HM, Vázquez OT, McGonagle D, Bydder G, Santer RM, Benjamin M. Development of the human Achilles tendon enthesis organ. *J Anat*. 2008; 213(6): 718-24. doi: 10.1111/j.1469-7580.2008.00997.x.
4. Kachlik D, Baca V, Cepelik M, Hajek P, Mandys V, Musil V, Skala P, Stingl J. Clinical anatomy of the retrocalcaneal bursa. *Surg Radiol Anat*. 2008; 30(4): 347-53. doi: 10.1007/s00276-008-0335-4.
5. Pirri C, Stecco C, Güvener O, Mezian K, Ricci V, Jačisko J, Fojtik P, Kara M, Chang KV, Dughbaj M, Özçakar L; EURO-MUSCULUS: European Musculoskeletal Ultrasound Study Group in Physical and Rehabilitation Medicine.. EURO-MUSCULUS/USPRM Dynamic Ultrasound Protocols for Ankle/Foot. Am J Phys Med Rehabil. 2024 Mar 1;103(3):e29-e34. doi: 10.1097/PHM.0000000000002349. Epub 2023 Oct 30. PMID: 37903600.
6. Ricci V, Ricci C, Gervasoni F, Giulio C, Farì G, Andreoli A, Özçakar L. From physical to ultrasound examination in lymphedema: a novel dynamic approach. J Ultrasound. 2022 Sep;25(3):757-763. doi: 10.1007/s40477-021-00633-4. Epub 2022 Jan 9. PMID: 35000129; PMCID: PMC9402863.

7. Cocco G, Ricci V, Corvino A, Abate M, Vaccaro A, Bernabei C, Cantisani V, Vallone G, Caiazzo C, Caulo M, Pizzi AD. Musculoskeletal disorders in padel: from biomechanics to sonography. J Ultrasound. 2024 Apr 5. doi: 10.1007/s40477-023-00869-2. Epub ahead of print. PMID: 38578364.
8. Cocco G, Ricci V, Villani M, Delli Pizzi A, Izzi J, Mastandrea M, Boccatonda A, Naňka O, Corvino A, Caulo M, Vecchiet J. Ultrasound imaging of bone fractures. Insights Imaging. 2022 Dec 13;13(1):189. doi: 10.1186/s13244-022-01335-z. PMID: 36512142; PMCID: PMC9748005.
9. Mahan J, Damodar D, Trapana E, Barnhill S, Nuno AU, Smyth NA, Aiyer A, Jose J. Achilles tendon complex: The anatomy of its insertional footprint on the calcaneus and clinical implications. J Orthop. 2019 Jun 10;17:221-227. doi: 10.1016/j.jor.2019.06.008. PMID: 31889745; PMCID: PMC6931068.
10. Ballal MS, Walker CR, Molloy AP. The anatomical footprint of the Achilles tendon: a cadaveric study. Bone Joint J. 2014 Oct;96-B(10):1344-8. doi: 10.1302/0301-620X.96B10.33771. PMID: 25274919.

2.3 Dynamic Ultrasound Imaging for Insertional Achilles Tendinopathy: a Retrospective Observational Study

ABSTRACT

Objectives

Recently, a novel dynamic maneuver in which the retrocalcaneal soft tissues are squeezed (CoRi sign) has been described for the diagnosis of partial tears involving the deep fibers of the Achilles

tendon. This retrospective observational study aims to assess the prevalence of the CoRi sign in a cohort of patients with a clinical diagnosis of IAT.

Methods

A consecutive cohort of 58 patients (32 males, 26 females) seen at our institution with a clinical diagnosis of IAT comprised the study group for a retrospective observational study to assess the prevalence of the CoRi sign in the study population and to correlate the findings on static B-mode and color/power Doppler sonography with the CoRi dynamic maneuver.

Results

The prevalence of CoRi sign was 15,5% in the study cohort (9/58) and 26,4% (9/34) in the subgroup of IAT patients with bursal effusion in B-mode coupled with synovial hyperemia of in color/power Doppler. Of the 9 patients with a positive dynamic maneuver, 8 of them presented insertional tendinosis with intra-tendinous hyperemia at color/power Doppler; in addition, none showed Achilles bone spurs of the calcaneal tuberosity. Lastly, 4 of the 9 patients with a positive CoRi sign showed tendon-bone junction hyperemia in the absence of a bone spur.

Conclusions

Tendon undersurface disruption in IAT patients is not uncommon and dynamic ultrasound imaging is a valuable for diagnosis. Hyperemic retrocalcaneal bursitis, insertional tendinosis with intra-tendinous hyperemia, and tendon-bone junction hyperemia are the most common static sonographic findings respectively in CoRi-positive patients.

Level of Evidence Level IV – Retrospective Observational Study

Keywords:

Achilles tendon, dynamic, ultrasound, sonography, bursa, color Doppler

ABBREVIATIONS

IAT: insertional Achilles tendinopathy, AT: Achilles tendon, CoRi: Cocco-Ricci sign, MRI: magnetic resonance imaging

INTRODUCTION

Insertional Achilles tendinopathy (IAT) is a clinical entity defined by pain and swelling at the calcaneal attachment of the Achilles tendon (AT). 1,2 In clinical practice, physical examination of the hindfoot is coupled with ultrasound assessment of the tendon and its insertion at the posterior surface of the calcaneus. 3 The most common static sonographic findings of IAT in B-mode are focal tendinosis with or without intra-tendinous calcifications, enthesophyte of the calcaneal tuberosity (bone spur), and synovial hypertrophy of the deep retrocalcaneal bursa (located between the Achilles tendon and the Kager's fat pad). 4,5,6 In addition, color and power Doppler is performed to assess the hyperemia and hypervascularization of the aforementioned anatomic structures of the hindfoot. 4,5,6

Recently, a novel dynamic ultrasound sign in IAT patients has been described as the Cocco-Ricci (CoRi) sign to improve the diagnosis of partial tears involving the deep fibers of the AT. 7 Indeed, IAT is a peculiar type of tendon injury that is often not visible with a static sonographic examination because the distal AT is apposed to the posterior surface of the calcaneus; a manual squeeze of retrocalcaneal bursal effusion may be necessary to push the anechoic fluid within the disruption of the tendon undersurface rendering the tear more visible.

The first aim of our retrospective observational study is to assess the prevalence of the CoRi sign in a cohort of patients with a clinical diagnosis of IAT. Secondly, we hypothesize that insertional tendinosis of AT with intra-tendinous hyperemia and potential mechanical impingement with the underlying bone tissue is more often associated with a positive CoRi sign than a sonographic pattern with bone spur involving the tendon-bone junction.

MATERIALS & METHODS

Patients selection

This retrospective observational study involved patients with a clinical diagnosis of IAT who were referred to the Institute for Advanced Biomedical Technologies, Gabriele d'Annunzio University of Chieti, Italy, for sonography that was performed between June 2024 and December 2024. The clinical diagnosis of IAT was provided by the referring clinicians—orthopedic surgeons, rheumatologists, PM&R physicians, and sports medicine physicians—operating in the Gabriele d'Annunzio University Hospital. The study did not require approval by The Ethical Committee of Gabriele d'Annunzio University of Chieti and Pescara considering the retrospective analysis of anonymized data routinely collected during daily practice. The study was conducted in accordance with the Declaration of Helsinki. The inclusion criteria were clinical findings of tenderness and swelling at the insertion of the AT at the calcaneus, as documented in the medical record, an age of at least 18 years, and an X-ray excluding fractures of the calcaneal bone performed within 30 days before the ultrasound assessment. Previous surgical procedures of the ankle or hindfoot, previous injection of the AT, age less than 18 years, rheumatological disorders, endocrinological pathologies potentially involving the AT, and major traumas of the foot were defined as exclusion criteria. All subjects gave their informed consent for inclusion before they participated in the

study. The authors confirm that the data supporting the findings of this study are available within the article [and/or] its supplementary materials. The age and gender of each patient was recorded.

Sonographic protocol

Ultrasound equipment and patient positioning

The ultrasound images and videos had been originally acquired using the i18LX5 high-frequency transducer, Canon Aplio I800, Canon Medical Systems, Shimo Ishigami, Otawara-Shi, Japan. The patients had been examined in the prone position, with the ankle joint in neutral position and the foot hanging over the edge of the bed. A large amount of acoustic gel between the transducer and the heel skin was used to avoid an unintentional squeeze of the superficial tissues over the calcaneus. All of the ultrasound examinations included in the study were performed by a medical doctor (G.C.) with more than 15 years of experience in musculoskeletal ultrasound. Subsequently, a different medical doctor (V.R.) with more than 10 years of experience in musculoskeletal ultrasound retrospectively reviewed both the static ultrasound images and the dynamic sonographic videos acquired by the first sonographer for the purposes of this study.

Static ultrasound imaging

To visualize the AT attaching to the posterior surface of the calcaneal tuberosity, the transducer was positioned in the longitudinal plane. [8] Shifting the probe from the midline to the medial and lateral parasagittal planes assessed the entire width of the retrocalcaneal region. Then, rotating the probe 90 degrees, the same anatomical site was visualized in a transverse plane from proximal to distal. The presence or absence of insertional tendinosis, bone spur, intra-tendinous calcifications, and retrocalcaneal bursitis was assessed during the B-mode ultrasound examination of the patients **(Figure 1)**. Likewise, the presence or absence of intra-tendinous hyperemia,

tendon-bone junction hyperemia, peri-calcific hyperemia, and synovial hyperemia involving the retrocalcaneal bursa was evaluated with the color and power Doppler imaging **(Figure 2)**. The authors collected the presence or absence of blood flows at the different anatomic compartments of the hindfoot, but there was no quantitative or semi-quantitative grading of the vascular signals.

Dynamic ultrasound imaging

As described by Cocco and Ricci, a dynamic ultrasound assessment of the retrocalcaneal region was performed to identify the presence or absence of the CoRi sign. [7] With one hand holding the transducer over the posterior surface of the heel, the other hand was used to compress the deep retrocalcaneal region by gently pinching the soft tissues between the thumb and the index finger **(Video 1)**. In patients with shifting of bursal effusion inside the focal disruption of the tendon undersurface during the dynamic maneuver, the CoRi sign was defined as positive **(Figure 3)**. The presence or absence of the CoRi sign during the dynamic maneuver was correlated with the static ultrasound imaging findings.

RESULTS

Study cohort

From the initial study population of 64 patients, 4 were excluded due to age less than 18 years and 2 patients were excluded due to previous surgical interventions at the AT. The study cohort therefore consisted of 58 patients, with a mean age of 54 years (54 ± 11,72). The gender distribution was 32 males (55%) and 26 females (45%).

Static ultrasound imaging

As regards the B-mode sonographic findings, the insertional tendinosis, bone spur, intra-tendinous calcifications, and retrocalcaneal bursitis were identified in 58/58 (100%), 19/58 (32,7%), 44/58 (75,8%), and 34/58 (58,6%) respectively **(Supplementary Table 1)**. Likewise, intra-tendinous hyperemia, tendon-bone junction hyperemia, peri-calcific hyperemia, and synovial hyperemia of the retrocalcaneal bursa were identified in 55/58 (94,8%), 23/58 (39,6%), 41/58 (70,6%), and 34/58 (58,6%) during the color and power Doppler examination respectively.

All the patients with retrocalcaneal bursitis in B-mode (34/58) showed synovial hyperemia of the bursal walls with the color/power Doppler. Hyperemia of the tendon-bone junction (23/58) was found in patients with and without bone spurs. There were 19/58 patients who had a bone spur of the calcaneus and hyperemia at the tendon-bone junction hyperemia; only 4/58 patients had tendon-bone junction hyperemia without a bone spur.

Dynamic ultrasound imaging

Performing the dynamic compression of the retrocalcaneal space 9/58 patients (15,5% of the study cohort) presented a positive CoRi sign **(Supplementary Table 1)** with an abnormal spilling of the bursal effusion within the focal discontinuity of the deep tendon fibers. Considering the subgroup of IAT patients with bursal effusion in B-mode and hyperemia of its synovial walls in color/power Doppler, the prevalence of a positive dynamic maneuver is 26,4% (9/34). All 9 patients with a positive CoRi sign were male. None of the 9 patients with a positive dynamic ultrasound maneuver due to focal disruption of the tendon undersurface presented a bone spur of the calcaneal tuberosity in B-mode. Lastly, tendon-bone junction hyperemia without a bone spur was identified in 4 of the 9 patients with a positive CoRi sign (4/9, 44,4%) **(Supplementary Table 1)**.

DISCUSSION

Achilles tendon disorders are common in daily practice and may involve the midportion or the insertional segment at the calcaneal attachment. [1,2] The midportion Achilles tendinopathy usually presents with a fusiform in-shape tendon thickening, eventually coupled with inflammatory changes and adhesions of the surrounding non-synovial sheath (i.e., Achilles para-tendinopathy). [4,9] In contrast, the insertional Achilles tendinopathy encompasses a wide spectrum of histological changes involving the tendon, the fibrocartilage plate of the tendon-bone junction, the calcaneal tuberosity, the retrocalcaneal bursa, the Kager's fat pad, and the superficial retrocalcaneal bursae. [10,11]

High-resolution ultrasound imaging is commonly used in clinical practice to assess the Achilles tendon [12,13] and, more recently, dynamic sonographic protocols of the ankle and foot have been proposed to optimize the diagnosis of tricky conditions such as tendon delamination or, focal avulsion of the collagen fibers from the fibrocartilaginous footprint. [7,14]

To the best of our knowledge, this is the first retrospective observational study correlating static and dynamic high-resolution sonography of a cohort of IAT patients. For IAT patients with static sonographic findings of *hyperemic retrocalcaneal bursitis*, the dynamic assessment plays a crucial role in their management by taking advantage of the bursal effusion as a natural contrast agent to diagnose partial tear of the deep fibers of the Achilles tendon.

Indeed, if in patients with isolated retrocalcaneal bursitis, an ultrasound-guided injection of the bursa with corticosteroid can be considered among the suitable interventional procedures, in patients with disruption of the tendon's undersurface coupled with the bursal pathology, this injection should be avoided to prevent the potential leaking of corticosteroid inside the tendon

tissue. [15,16] In patients with a positive CoRi sign alternative mixtures such as hyaluronic acid or ortho biological agents may be considered for injecting the bursal cavity and/or the Achilles tendon undersurface. [17,18,19] Some authors have also proposed a percutaneous ultrasonic device to perform, under ultrasound guidance, a retrocalcaneal bursectomy coupled with a local debridement of the tendon-fat interface to promote healing of the tendon undersurface in a study population of 34 IAT patients (40 procedures) recalcitrant to the conservative treatments. [20]

Moreover, in patients with a positive CoRi sign secondary to disruption of the Achilles tendon undersurface, the rehabilitation approach can be tailored by avoiding excessive stretching, modifying exercise therapy, and offering heel lifts to reduce the intra-tendinous pressure. Indeed, biomechanical studies have demonstrated that the intra-tendinous pressure increases exponentially especially in the deep insertional region of the Achilles tendon during the eccentric heel-drop. [21,22,23] In IAT patients with a positive Cori sign, we speculate that a safe zone to apply tensile forces could be an ankle range of motion between -15° and 0° that promotes tendon healing but prevents a compressive overload against the posterior surface of the calcaneus. [21,22,23]

Hypervascularization of the degenerated deep fibers of the AT is a static sonographic sign more frequently related to discontinuity of the tendon undersurface visualized with the dynamic maneuver compared to the bony overgrowth of the tendon-bone junction. This sonographic finding confirms the pathomechanical mechanism of repetitive compression of the tendon against the superior facet of the calcaneal tuberosity as previously demonstrated in the pertinent literature with biomechanical investigations. [21,22,23]

The main limitation of the present study is the absence of a surgical exploration to acquire a gross anatomical demonstration of the tendon undersurface's disruption depicted during the dynamic sonographic assessment. Indeed, considering the favorable clinical and functional outcomes of patients with a focal injury of deep fibers of the AT managed with conservative approaches

(orthosis, rehabilitation techniques, etc), there is no indication for surgery in these patients. Lastly, a correlation between dynamic sonography and MRI to assess the potential of the two different techniques in diagnosing tendon undersurface disruption may be considered a further step forward to define the most appropriate diagnostic pathway for this challenging pathological condition.

CONCLUSION

Disruption of deep fibers of AT in IAT patients is a challenging condition to diagnose and, dynamic ultrasound imaging is a valuable tool to optimize the management of these patients in clinical practice. Based on our retrospective observational investigation, hyperemic retrocalcaneal bursitis, insertional tendinosis with intra-tendinous hyperemia, and tendon-bone junction hyperemia are respectively the most common static sonographic findings in CoRi-positive patients.

Supplementary Table 1.

Demographic features of the study cohort and static/dynamic sonographic findings.

N	Age	Gender	IT / ITH	BS / TBJH	ITC / PCH	RCB / SH	CoRi
1	57	M	+ +	- -	- -	- -	-
2	61	F	+ +	+ +	+ +	+ +	-
3	43	F	+ -	- -	+ -	- -	-

4	57	F	+ +	- -	+ +	- -	-
5	46	F	+ +	- -	+ +	+ +	-
6	58	M	+ +	- +	+ +	+ +	+
7	69	M	+ +	- +	+ +	+ +	+
8	51	M	+ +	- -	- -	- -	-
9	60	M	+ +	+ +	+ +	+ +	-
10	56	F	+ +	+ +	+ +	- -	-
11	31	M	+ +	- -	+ +	- -	-
12	58	M	+ +	- -	+ +	+ +	-
13	54	F	+ +	- -	- -	+ +	-
14	58	F	+ +	+ +	+ +	- -	-
15	37	F	+ +	- -	+ +	- -	-
16	60	F	+ +	+ +	+ +	+ +	-
17	56	F	+ +	+ +	+ +	- -	-
18	68	M	+ +	+ +	+ +	+ +	-
19	21	M	+	-	-	-	-

			+	-	-	-	
20	62	M	+ +	- -	+ +	+ +	+
21	62	M	+ +	+ +	+ +	+ +	-
22	55	M	+ +	- -	+ +	+ +	-
23	65	M	+ +	- -	- -	+ +	+
24	51	F	+ +	+ +	- -	+ +	-
25	64	M	+ +	- -	- -	+ +	+
26	58	M	+ +	- -	- -	- -	-
27	63	F	+ +	+ +	+ +	+ +	-
28	42	F	+ +	- -	+ -	- -	-
29	58	F	+ +	- -	+ +	- -	-
30	41	F	+ -	- -	+ +	+ +	-
31	62	M	+ +	- +	+ +	+ +	+
32	73	M	+ +	- +	+ +	+ +	+
33	49	M	+ +	- -	- -	- -	-
34	58	F	+ +	+ +	+ +	+ +	-

35	57	F	+ +	+ +	+ +	- -	-
36	31	M	+ +	- -	+ +	- -	-
37	62	M	+ +	- -	+ +	+ +	-
38	50	F	+ +	- -	- -	+ +	-
39	59	F	+ +	+ +	+ +	- -	-
40	35	F	+ +	- -	+ +	- -	-
41	59	F	+ +	+ +	+ +	+ +	-
42	56	M	+ +	+ +	+ +	- -	-
43	70	M	+ +	+ +	+ +	+ +	-
44	20	F	+ +	- -	- -	- -	-
45	61	M	+ +	- -	+ +	+ +	-
46	63	M	+ +	+ +	+ +	+ +	-
47	59	M	+ +	- -	+ +	+ +	-
48	66	M	+ +	- -	+ +	+ +	+
40	52	M	+ +	+ +	- -	+ +	-
50	64	M	+	-	+	+	-

			+	-	+	+	
51	57	M	+ +	- -	- -	- -	-
52	62	F	+ +	+ +	+ +	+ +	-
53	41	F	+ +	- -	+ -	- -	-
54	57	F	+ +	- -	+ +	- -	-
55	42	M	+ -	- -	+ +	+ +	+
56	31	M	+ +	- -	+ +	- -	-
57	63	M	+ +	- -	+ +	+ +	-
58	51	F	+ +	- -	- -	+ +	-

M: male, F: female, IT: insertional tendinosis, ITH: intra-tendinous hyperemia, BS: bone spur, TBJH: tendon-bone junction hyperemia, ITC: intra-tendinous calcification, PCH: peri-calcific hyperemia, RCB: retrocalcaneal bursitis, SH: synovial hyperemia, CoRi: Cocco-Ricci sign, +: presence, -: absence

DECLARATION SECTIONS

Ethics Approval

The study did not require approval by The Ethical Committee of Gabriele d'Annunzio University of Chieti and Pescara considering the retrospective analysis of anonymized data routinely collected during daily practice. The study was conducted in accordance with the Declaration of Helsinki.

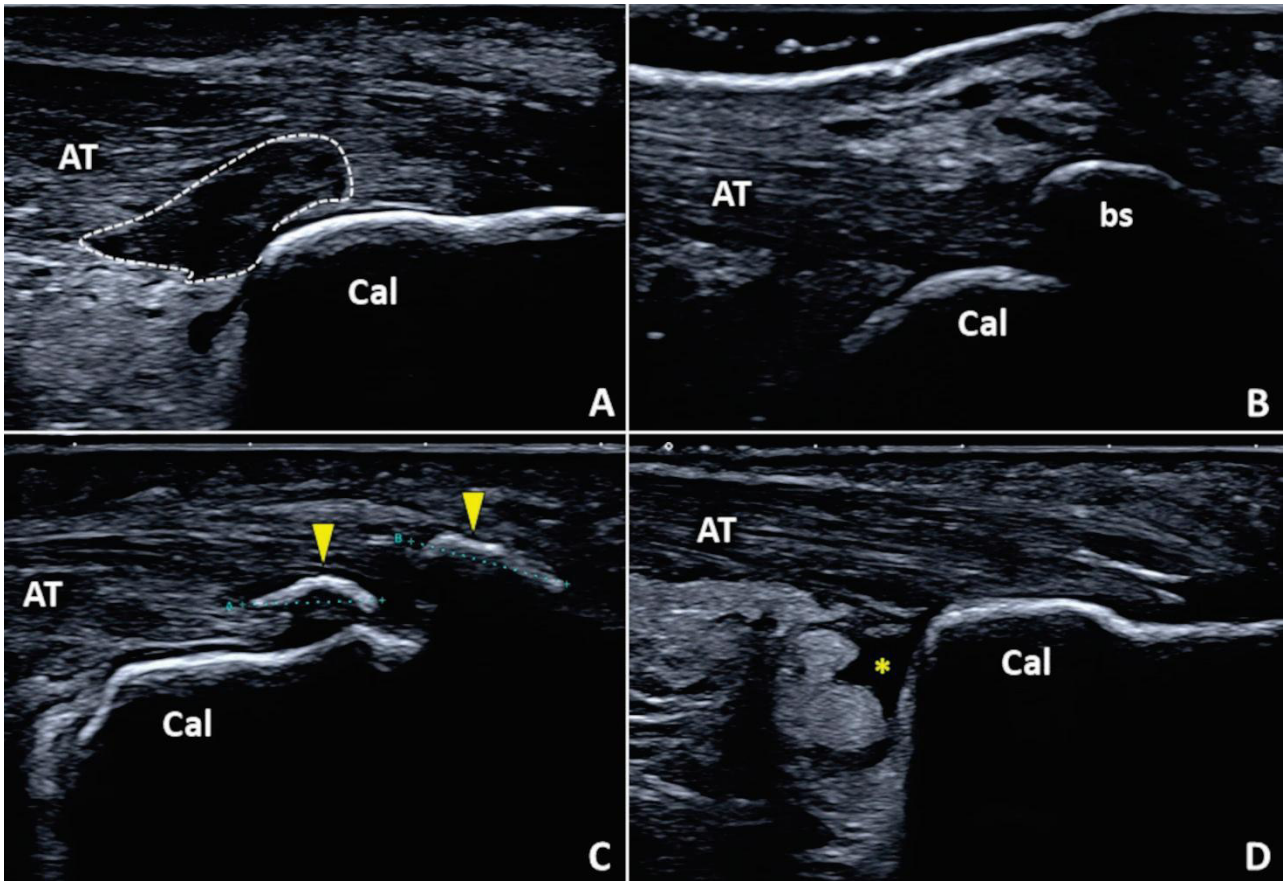
Consent to Partecipate

All subjects gave their informed consent for inclusion before they participated in the study. The study was conducted in accordance with the Declaration of Helsinki.

Figure legends.

Figure 1.

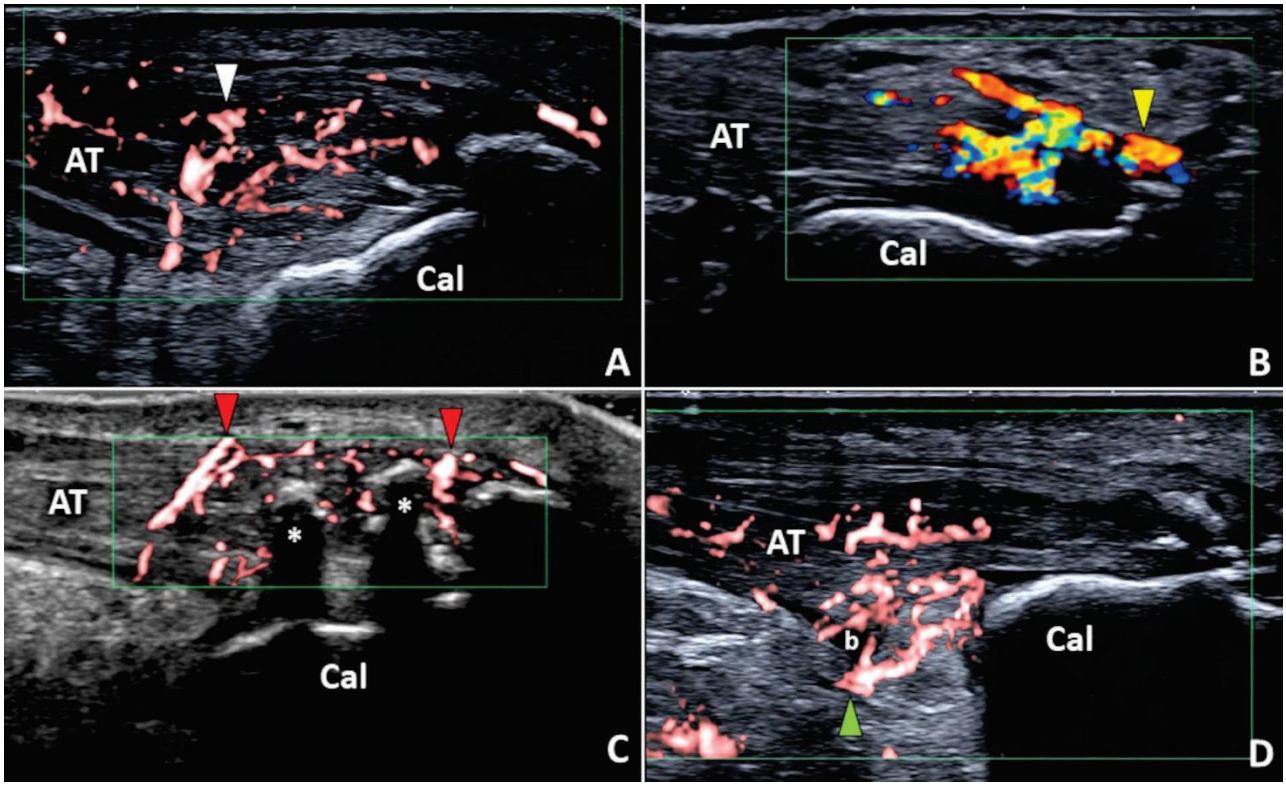
Static B-mode sonographic features of the IAT.



Positioning the transducer in a longitudinal plane along the Achilles tendon *(AT)* and the calcaneus *(Cal)*, the four elementary lesions - insertional tendinosis *(white dotted line)* **(A)**, bone spur *(bs)* **(B)**, intra-tendinous calcification *(yellow arrowhead)* **(C)**, and retrocalcaneal bursitis *(yellow asterisk)* **(D)** - can be accurately assessed in IAT patients.

Figure 2.

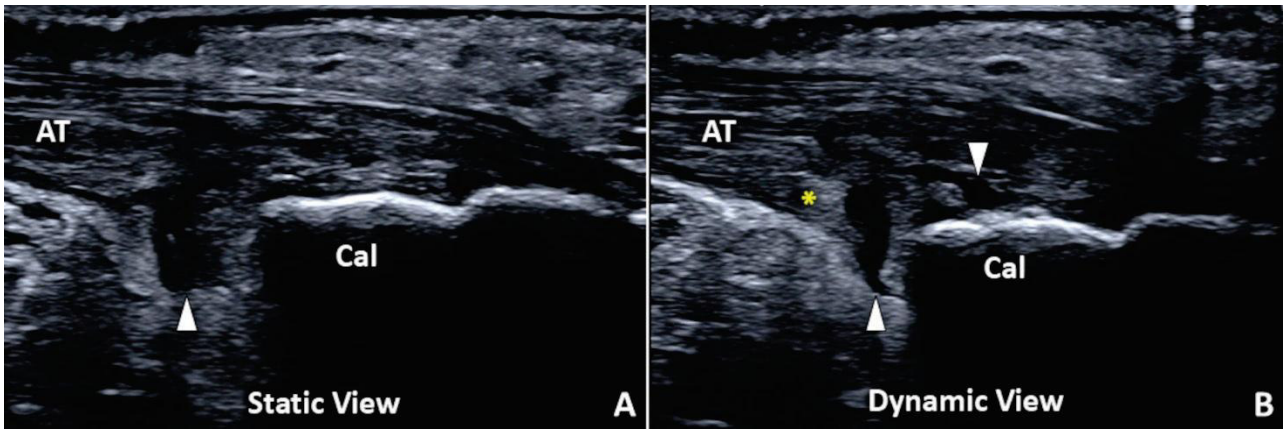
Static color/power Doppler sonographic features of the IAT.



Positioning the transducer in a longitudinal plane along the Achilles tendon *(AT)* and the calcaneus *(Cal)*, the four elementary lesions – intra-tendinous hyperemia *(white arrowhead)* **(A)**, tendon-bone junction hyperemia *(yellow arrowhead)* **(B)**, peri-calcific hyperemia *(red arrowheads)* **(C)**, and synovial hyperemia of the retrocalcaneal bursa *(green arrowhead)* **(D)** - can be accurately assessed in IAT patients. white asterisks: intra-tendinous calcifications, b: retrocalcaneal bursa

Figure 3.

Dynamic ultrasound imaging for the IAT – the CoRi sign.



Starting from a static longitudinal view of the Achilles tendon *(AT)* **(A)**, the bursal effusion *(white arrowheads)* can be manually pushed within the focal disruption of the tendon's undersurface by pinching the soft tissues of the retrocalcaneal space **(B)**. Cal: calcaneus, yellow asterisk: proximal stump of the tendon fibers

Video legends.

Video 1.

Positive CoRi sign shows the partial tear involving the deep fibers of the Achilles tendon during the dynamic maneuver.



Video 1.avi

References

1. Krishna Sayana M, Maffulli N. Insertional achilles tendinopathy. *Foot Ankle Clin*. 2005; 10(2): 309-20. doi: 10.1016/j.fcl.2005.01.010.

2. van Dijk CN, van Sterkenburg MN, Wiegerinck JI, et al. Terminology for achilles tendon related disorders. *Knee Surg Sports Traumatol Arthrosc*. 2011; 19(5): 835-41. doi: 10.1007/s00167-010-1374-z.

3. Ricci V, Özçakar L. Life after ultrasound: are we speaking the same (or a new) language in physical and rehabilitation medicine? *J Rehabil Med*. 2019; 51(3): 234-235. doi: 10.2340/16501977-2527.

4. Cocco G, Ricci V, Corvino A, et al. Musculoskeletal disorders in padel: from biomechanics to sonography. *J Ultrasound*. 2024 Apr 5. doi: 10.1007/s40477-023-00869-2. Epub ahead of print. PMID: 38578364.

5. Lindén L, Granath M, Hedlund P, Spang C, Alfredson H. Ultrasonography- and doppler-guided surgical treatment for insertional achilles tendinopathy: results from a case series in a southern sweden county hospital. *Foot Ankle Orthop*. 2023; 8(1): 24730114231165014. doi: 10.1177/24730114231165014.

6. Weidermann F, Hirschmüller A, Tamborrini G. CME sonografie 108: die achillessehne im ultraschall: sonoanatomie und pathologien CME-fragen [CME sonography 108: achilles tendon ultrasound:

sonoanatomy and pathologies]. *Praxis (Bern 1994).* 2023; 112(4): 271-282. German. doi: 10.1024/1661-8157/a004032.

7. Cocco G, Ricci V. Dynamic ultrasound assessment for insertional achilles tendinopathy: the COcco-RIcci (CORI) sign. *Skeletal Radiol*. 2024 Jul 10. doi: 10.1007/s00256-024-04746-9.

8. Özçakar L, Kara M, Chang KV, Bayram Çarli A, Hung CY, Tok F, Wu CH, Akkaya N, Hsiao MY, Tekin L, Wang TG, Ulaşlı AM, Chen WS, De Muynck M. EURO-MUSCULUS/USPRM. Basic scanning protocols for ankle and foot. *Eur J Phys Rehabil Med*. 2015; 51(5): 647-53.

9. Ricci V, Mezian K, Chang KV, Tamborrini G, Jačisko J, Naňka O, Özçakar L. Ultrasound-guided injection of the achilles paratenon: a cadaveric investigation. *Foot Ankle Surg*. 2024; 30(4): 313-318. doi: 10.1016/j.fas.2024.01.005.

10. Ricci V, Cocco G, Mezian K, Chang KV, Tamborrini G, Naňka O, Özçakar L. Histo-anatomy and sonographic examination for the retrocalcaneal bursal complex: EURO-MUSCULUS/USPRM approach. *J Ultrasound Med*. 2024; 43(11): 2027-2038. doi: 10.1002/jum.16544.

11. Ricci V, Chang KV, Naňka O, Özçakar L. Superficial retrocalcaneal bursae and nerves: from anatomy to ultrasound-guided procedures. *Clin Anat*. 2024 Jun 11. doi: 10.1002/ca.24193.

12. Bertolotto M, Perrone R, Martinoli C, Rollandi GA, Patetta R, Derchi LE. High resolution ultrasound anatomy of normal achilles tendon. *Br J Radiol*. 1995; 68(813): 986-91. doi: 10.1259/0007-1285-68-813-986.

13. Filippucci E, Aydin SZ, Karadag O, Salaffi F, Gutierrez M, Direskeneli H, Grassi W. Reliability of high-resolution ultrasonography in the assessment of achilles tendon enthesopathy in seronegative spondyloarthropathies. *Ann Rheum Dis*. 2009; 68(12): 1850-5. doi: 10.1136/ard.2008.096511.

14. Pirri C, Stecco C, Güvener O, Mezian K, Ricci V, Jačisko J, Fojtik P, Kara M, Chang KV, Dughbaj M, Özçakar L; EURO-MUSCULUS: european musculoskeletal ultrasound study group in physical and

rehabilitation medicine.. EURO-MUSCULUS/USPRM Dynamic ultrasound protocols for ankle/foot. *Am J Phys Med Rehabil*. 2024; 103(3): e29-e34. doi: 10.1097/PHM.0000000000002349.

15. Turmo-Garuz A, Rodas G, Balius R, Til L, Miguel-Perez M, Pedret C, et al. Can local corticosteroid injection in the retrocalcaneal bursa lead to rupture of the achilles tendon and the medial head of the gastrocnemius muscle? *Musculoskelet Surg*. 2014; 98(2): 121-6. doi: 10.1007/s12306-013-0305-9.

16. Pękala PA, Henry BM, Pękala JR, Piska K, Tomaszewski KA. The Achilles tendon and the retrocalcaneal bursa: an anatomical and radiological study. *Bone Joint Res*. 2017; 6(7): 446-451. doi: 10.1302/2046-3758.67.BJR-2016-0340.R1. Erratum in: *Bone Joint Res*. 2019 Oct 3;8(9):437. doi: 10.1302/2046-3758.88.BJR-2016-0340.R1.

17. Ohana N, Segal D, Kots E, Feldman V, Nyska M, Palmanovich E, Slevin O. A pilot study exploring the use of hyaluronic acid in treating insertional achilles tendinopathy. *J Orthop Surg (Hong Kong)*. 2024; 32(1): 10225536241242086. doi: 10.1177/10225536241242086.

18. Ferreira GF, Caruccio FRC, Guerrero Bou Assi JR, Pedroso JP, Dos Santos TF, Arliani GG, Filho MVP. Ultrasound-guided hyaluronic acid injection for the treatment of insertional achilles tendinopathy: a prospective case series. *Foot Ankle Surg*. 2022; 28(7): 879-882. doi: 10.1016/j.fas.2021.12.004.

19. Lo Presti M, Costa GG, Agrò G, Vasco C, Zunarelli P, Zaffagnini S. Adipose-derived stromal vascular fraction injection in a competitive high-level athlete affected by insertional achilles tendinopathy. *J Foot Ankle Surg*. 2021; 60(3): 626-629. doi: 10.1053/j.jfas.2020.04.019.

20. Chimenti RL, Stover DW, Fick BS, Hall MM. Percutaneous ultrasonic tenotomy reduces insertional achilles tendinopathy pain with high patient satisfaction and a low complication rate. *J Ultrasound Med*. 2019; 38(6): 1629-1635. doi: 10.1002/jum.14835.

21. Pringels L, Vanden Bossche L, Wezenbeek E, Burssens A, Vermue H, Victor J, Chevalier A. Intratendinous pressure changes in the achilles tendon during stretching and eccentric loading:

implications for Achilles tendinopathy. *Scand J Med Sci Sports*. 2023; 33(5): 619-630. doi: 10.1111/sms.14285.

22. Pringels L, Cook JL, Witvrouw E, Burssens A, Vanden Bossche L, Wezenbeek E. Exploring the role of intratendinous pressure in the pathogenesis of tendon pathology: a narrative review and conceptual framework. *Br J Sports Med*. 2023; 57(16): 1042-1048. doi: 10.1136/bjsports-2022-106066.

23. Pringels L, Stouthandel M, Van Hoof T, Martens M, Chevalier A, Burssens A, Wezenbeek E, Vanden Bossche L. Intratendinous pressure of the achilles tendon during exercise is related to the degree of tendon torsion. *Scand J Med Sci Sports*. 2023; 33(11): 2230-2238. doi: 10.1111/sms.14467.

3. Lavori scientifici pubblicati:

1- Cocco G, Ricci V, Ricci C, Naňka O, Catalano O, Corvino A, Boccatonda A, Serafini FL, Izzi J, Vallone G, Cantisani V, Iannetti G, Caulo M, Ucciferri C, Vecchiet J, Pizzi AD. Ultrasound imaging of the axilla. Insights Imaging. 2023 May 11;14(1):78. doi: 10.1186/s13244-023-01430-9. PMID: 37166516; PMCID: PMC10175532.

2- Cocco G, Ricci V, Villani M, Delli Pizzi A, Izzi J, Mastandrea M, Boccatonda A, Naňka O, Corvino A, Caulo M, Vecchiet J. Ultrasound imaging of bone fractures. Insights Imaging. 2022 Dec 13;13(1):189. doi: 10.1186/s13244-022-01335-z. PMID: 36512142; PMCID: PMC9748005.

3- Analay P, Kara M, Abdulsalam AJ, Yalçınkaya B, Ricci V, Cocco G, Naňka O, Özçakar L. Ultrasound Imaging and Guidance for Plantar Fascia Lesions: EURO-MUSCULUS/USPRM Approach. J Ultrasound Med. 2025 Aug;44(8):1509-1518. doi: 10.1002/jum.16694. Epub 2025 Mar 28. PMID: 40152055.

4- Ricci V, **Cocco G**, Mezian K, Chang KV, Barbosa J, Naňka O, Özçakar L. Patellar tendon-Hoffa fat pad interface: From anatomy to high-resolution ultrasound imaging. Knee. 2025 Jan;52:139-146. doi: 10.1016/j.knee.2024.10.024. Epub 2024 Nov 21. PMID: 39577112.

5- **Cocco G**, Ricci V, Corvino A, Abate M, Vaccaro A, Bernabei C, Cantisani V, Vallone G, Caiazzo C, Caulo M, Pizzi AD. Musculoskeletal disorders in padel: from biomechanics to sonography. J Ultrasound. 2024 Jun;27(2):335-354. doi: 10.1007/s40477-023-00869-2. Epub 2024 Apr 5. PMID: 38578364; PMCID: PMC11178742.

6- **Cocco G**. Dynamic color Doppler assessment for the detection of small abdominal hernias: the "Cocco Sign". J Ultrasound. 2025 Jul 4. doi: 10.1007/s40477-025-01048-1. Epub ahead of print. PMID: 40615770.

7- **Cocco G**, Ricci V, Corvino A, Pacini P, Boccatonda A, Naňka O, Sensi SL, Caulo M, Delli Pizzi A. Ultrasound Imaging of the Sciatic Nerve. Ultraschall Med. 2023 Oct;44(5):e263-e273. English. doi: 10.1055/a-2095-2842. Epub 2023 Oct 13. PMID: 37832532.

8- **Cocco G**, Ricci V. Dynamic ultrasound assessment for insertional achilles tendinopathy: the COcco-RIcci (CORI) sign. Skeletal Radiol. 2024 Jul 10. doi: 10.1007/s00256-024-04746-9. Epub ahead of print. PMID: 38987412.

9- Ricci V, Omodani T, Chang KV, Ricci C, Naňka O, Corvino A, Caulo M, Delli Pizzi A, Cantisani V, Tamborrini G, Özçakar L, **Cocco G**. Ultrasound Imaging/Guidance for Insertional Achilles Tendinopathy. Br J Radiol. 2025 Sep 16:tqaf231. doi: 10.1093/bjr/tqaf231.

4. Partecipazioni a congressi:

- Relatore al corso di aggiornamento: “La tecnologia al servizio della semeiotica: il ruolo dell’ecografia”. Ordine provinciale dei Medici e odontoiatri di Pescara. L’ecografia muscolo-tendinea. Presso Auditorium Petruzzi Via delle Caserme Pescara. 23 Novembre 2023

- Relatore al Corso teorico-pratico di ecografia muscolo-scheletrica 7-9 settembre 2023 presso Sicilì di Morigerati (SA)
- Relatore al corso di formazione di Ultrasonologia SIUMB di Palermo, programma formativo SIUMB Maggio 2023.
- Relatore al corso di formazione di Ultrasonologia SIUMB di Roma, programma formativo SIUMB Novembre 2023.
- Relatore al corso di formazione di Ultrasonologia SIUMB di Bologna, programma formativo SIUMB Maggio 2024.
- Relatore al corso di formazione di Ultrasonologia SIUMB di Campobasso, programma formativo SIUMB Settembre 2024
- Partecipazione al “4th International Workshop for Nerve & MSK Sonography” a Roma 15-16 Marzo 2024.
- Relatore al corso di formazione di Ultrasonologia SIUMB/Euroson di Napoli, Ottobre 2024
- Relatore al corso di formazione di Ultrasonologia SIUMB di Bologna, Maggio 2025
- Relatore al corso di formazione di Ultrasonologia e al Congresso XXX edizione SIUMB di Roma, Novembre 2025

5. Premi e riconoscimenti

- Premio per il miglior articolo di ecografia muscoloscheletrica (Palermo, SIUMB – maggio 2023), per l'articolo "Ultrasound imaging of bone fractures" (Cocco G. et al.), pubblicato su Insights into Imaging.
- Articolo più citato e scaricato 2023 sulla rivista Journal of Ultrasound: "Gallbladder polyps ultrasound: what the sonographer needs to know" (Cocco G. et al.).
- Top Cited Article 2022–2023 sulla rivista Clinical Case Reports. "Early detection of pleuro-pulmonary tuberculosis by bedside lung ultrasound: A case report and review of literature" (Cocco G. et al.).
- Highly Cited Paper 2024 sulla rivista Medicina Journal: "Atypical Sites of Lymphadenopathy after Anti-COVID-19 Vaccine: Ultrasound Features" (Cocco G. et al.).
- Highly Influential Paper 2024 del Journal of Ultrasound: "Musculoskeletal disorders in padel: from biomechanics to sonography" (Cocco G. et al.).
- Premio internazionale, ricevuto personalmente a Vienna nel febbraio 2025 durante l'ECR (European Congress of Radiology), per l'articolo "Ultrasound Imaging of the Axilla" (Cocco G. et al.), pubblicato su Insights into Imaging, premiato come "Most Downloaded Paper" 2024.

6. Conclusioni

Il percorso triennale di ricerca ha avuto come filo conduttore lo sviluppo e la valorizzazione dell'ecografia dinamica neuromuscoloscheletrica. I tre lavori principali che costituiscono il cuore di questa tesi hanno mostrato come la componente dinamica consenta di superare i limiti dell'approccio statico, integrando la valutazione morfologica con quella funzionale.

Lo studio sul Nervo Sciatico ha dimostrato l'utilità di un protocollo standardizzato con finestre anatomiche di riferimento, capace di migliorare la riproducibilità e l'accuratezza diagnostica nelle neuropatie da intrappolamento non discogeniche.

La descrizione e la validazione del segno CORI (Cocco-Ricci) per la tendinopatia inserzionale del tendine d'Achille hanno evidenziato come la dinamicità possa portare alla scoperta di nuovi reperti ecografici, capaci di arricchire il bagaglio semeiotico a disposizione. Infine, lo studio osservazionale retrospettivo ha confermato la rilevanza clinica di tali reperti, dimostrando che la dinamicità non è soltanto un esercizio descrittivo, ma uno strumento concreto per migliorare la diagnosi e orientare le scelte terapeutiche. In prospettiva, l'ecografia dinamica neuromuscoloscheletrica può aprire scenari di ricerca ancora inesplorati: dalla valutazione dei meccanismi di scorrimento e attrito tra strutture tendinee e nervose, allo studio delle interfacce miofasciali, fino alla personalizzazione dei percorsi riabilitativi attraverso un monitoraggio funzionale in tempo reale. In conclusione, la dinamicità ecografica si configura come un linguaggio diagnostico innovativo e in continua evoluzione, capace di arricchire l'imaging neuromuscoloscheletrico e non solo. Infatti, la mia ultima ricerca si è dedicata all'impiego dell'eco-color-Doppler nella diagnosi delle ernie della parete addominale durante la manovra dinamica di Valsalva e ha portato alla definizione del "Cocco Sign", ulteriore conferma del potenziale enorme che ha l'approccio ecografico dinamico nell'aprire nuove prospettive diagnostiche.

Chieti,

01/12/2025

TUTOR

Prof. Massimo Caulo



PhD Student

Dott. Giulio Cocco

